

# Reactive Power Compensation with DSTATCOM in different modes of operation of a Single Phase Micro grid

Ch. Rami Reddy<sup>1</sup>, B.V.Rajanna<sup>2</sup>, K. Harinadha Reddy<sup>3</sup>, K. V. Siva Reddy<sup>4</sup>, B. Prasanna Lakshmi<sup>5</sup>

<sup>1</sup> Dept. of Electrical and Electronics Engineering, Nalanda Institute of Engineering and Technology, Guntur, A. P.

<sup>2,4</sup> Dept. of Electrical and Electronics Engineering, KLEF, Vaddeswaram, Guntur, A. P., India

<sup>3</sup> Dept. of Electrical and Electronics Engineering, L B R College of Engineering, Krishna, A. P., India.

<sup>5</sup> Dept. of Electronics and communication Engineering, Nalanda Institute of Engineering and Technology, Guntur, A. P.  
crrreddy229@gmail.com<sup>1</sup> bv.rajanna@gmail.com<sup>2</sup> kadapa.hari@gmail.com<sup>3</sup> sivareddy.v.k@gmail.com<sup>4</sup>,  
prasanna@ngi.ac.in<sup>5</sup>

**Abstract:** This paper describes synchronized control of distribution static compensator (DSTATCOM) and distributed generators (DG) in a Micro grid. With large diffusion of distributed sources and system with single phase operation system may even have disturbance in voltage quite often if crosses the permissible limit. Reactive power compensation cannot be always possible with the devices having three phases at place of good position with the feeders physically spread out. Communication with DSTATCOM in a loop with a simple control strategy is proposed in this paper. The main factors like power flow in the line and the voltage sag are considered in the proposed reactive compensation technique. In order to moderate the reactive compensation, communication can be done to DSTATCOM with the help of feeders located at different points having the voltage and power flow in line. Maximum power which is actively available is provided by DGs and the reactive power compensation is done in the phase having shortage of reactive power with the help of single-phase DSTATCOM. In order to increase the reactive power inoculation ability of the DGs, the maximum available active power is fixed to a value lower than maximum active power during the permissible limit of the reactive power of the DG. In case of communication failure, a part of reactive compensation is always required by a primary control loop based on local measurement in the DSTATCOM. Permissible voltage regulation is observed and ensured in the proposed method. To validate the proposed method, presentation of analysis of data circulation of the communication scheme and power network and communication network closed loop simulation are done.

**Key words:** DSTATCOM, Micro grid, Reactive power compensation, Islanding mode, autonomous mode.

## 1. Introduction

Local power generation, power utility and

consumers can be benefited by micro grid formed by installation of distributed generators (DGs) [1]. Proper location of DG can increase the capacity of the feeders but does not mandatorily improve on power quality (PQ) or system reliability [2]. Some action must be initiated to make DG automatically improves system reliability [3]. Synchronized control of compensating devices and the DGs can be one of the key actions required. Reliable micro grid main objective is to maintain the PQ during power generation in both grid-connected and islanded mode. Detection and easing of the PQ events in a modern micro grid can be attained by power electronic device control and through compensation [4]. Poor voltage regulation in a micro grid caused by large diffusion of DGs is one of the major PQ problems. Voltage drop permissible limit is usually 10% in a micro grid [5]. Single-phase operation in a micro grid also involves the problem of voltage regulation. The major concern regarding PQ is increased by the micro sources having single phase in large number and single-phase converter-based DGs [6]. Feeders at the end usually have voltage regulation problem in a DGS having small capacity at photovoltaic rooftop position in a distribution network having lower voltage [7]. Voltage can be dropped below the permissible value on either side in a micro grid, with autonomous operations. So it is very essential for DGs and compensating devices to have synchronized parallel operation [8]. Control of voltage and load sharing in a micro grid is done by making the number of DGs operating in parallel by following various techniques of control proposed by the researchers [9]. Discussion in the control techniques which are decentralized is carried out for sharing of power and voltage support. Voltage support at fundamental frequency [10] can be

achieved by the converter providing real power to residential loads in city networks and reactive power injection into the grid [11]. Power regulation on the grid become more efficient and better by “source-following” strategy compared with “grid following” strategy as shown and observed in [12]. Droop control techniques always involve operation of converter just like the synchronous machine in a micro grid.

Island operation is also possible with them [13]. Voltage source converters (VSCs) are affected strongly by the grid impedance in the grid-connected case [14]. Thus, in a micro grid, the essential requirement for the DG control is customized or changed depending on connection of grid in grid-connected or island mode [15]. Implementations of purposefully-islanding and grid-connected operations of distributed power generation were done by proposing a control strategy in [16]. The influence of impedance in the line can be reduced with suitable choice of impedance at the output of the converter in decentralized parallel operation [17]. Investigation of resistive output impedance has a great influence on converter which is connected in parallel interfaced sources in an island micro grid in [18]. Demonstration of uninterruptible power supply system's parallel operation in a micro grid is done in [19]. Smart grid architecture for regulation of voltage in a decentralized, non hierarchal manner is proposed in [20]. To achieve energy management in real time, investigation of possibility in renewable sources is done with the help of parallel communication architecture [21]. Flexible communication scheme with distributed generation can help in finding solutions to a problem which is shown with a varied network [22]. Proper synchronization of DGs will provide communicated measurement with synchronized control of the DGs. In a micro grid, DGs involves different ways of synchronization techniques [23], [45]. At other harmonic frequencies considering other sequence components for grid-connected power converters, a new multi resonant frequency-adaptive synchronization method is proposed in [24]. Many residential consumers have many DGs operate with maximum power injections in single-phase distribution lines. Active power generation factor is considered for tax exception [25]. Participation of DGs in voltage regulation is not involved in the IEEE 1547 feeder [26]. Active voltage regulation at the point of common coupling (PCC) cannot be done by the Distributed Resources (DR) [IEEE 1547, section 4.1.1]”). An optional or an improvement of

the customary electric power system (EPS) is achieved by small scale power generation technologies such as DR systems [27]. By using a power electronic interface sometimes, they are connected to the grid. EPS area is connected to local EPS even at the permissible voltage limits at the PCC in which the DR cannot participate in the active voltage regulation specified in ANSI C84.1 Range A [28]. Reactive support with load growth by increasing the power rating of DGs is not always possible because of changes in device rating of power electronic device with utility converter interfaced DGs. Voltage support requirement and PQ enhancement can be provided by the distribution static compensator (DSTATCOM). Ease of variation in the positive and negative sequence voltages at the fundamental frequency and ride through capability during transients is provided by DSTATCOM is proposed in [29-30]. Voltage regulation in the network having lower voltages must consider both the active power and reactive power because they are strongly coupled [31]. In distribution system, compensation of reactive power and load unbalance are studied and well observed in [32]. With the help of synchronous reference frame method, the instantaneous reactive power method is covered. Electric distribution system having four wires for PQ enhancement is described in [33]. DSTATCOM involves a current-controlled voltage source inverter with a DC bus capacitor [34]. Supply power factor improvement, harmonic elimination, and load, terminal voltage improvement at the PCC and load balancing is done by the DSTATCOM [35]. PI controllers have the feedback signals provided by the DC bus voltage of the DSTATCOM and three-phase voltages at PCC. Either voltage or current control modes are involved in the operation of DSTATCOM [36]. Balanced sinusoidal voltage will be occurred at the distribution bus by the DSTATCOM in the voltage control mode. Harmonic distortion caused by the various loads will be eliminated in the current control mode. DSTATCOM and DGS must be operated in a voltage control mode in a micro grid to achieve reactive power harmonization. Compensation of reactive power cannot be possible frequently by the device having three phases operating in single-phase at suitable location in which the feeders are far apart in nature [37].

Communication infrastructure is a very essential requirement for exchange of information and coordinate control between the DGs and DSTATCOM. Power utility demands for distributed

energy resources are well maintained by increasing communication setup infrastructure [38]. The voltage improvement with DSTATCOM and DGs will be made possible easily by using communication infrastructure. In a low voltage network, the converters which are interfaced with micro sources and loads which are physically apart from each other with a total power consumption of 720-kW shared among three communities, each with several hundred domestic consumers provided by the off grid renewable connection at the Anangu Solar Station of South Australia [39]. Device current rating must consider supply reactive power and rated power supplied by the micro sources in this paper. The reactive power drawn by the DGs reach to the maximum limit and the voltage regulation falls below the permissible limit during a high loading period [40]. The reactive compensation must act

punctually with the voltage change due to the frequent change in load and continuous change in power generation of the DGs [41]. The voltage influence is caused mainly by the change in line power flow, so the adjustment of reactive compensation depending on line power flow will be profitable [42-45]. With the help of synchronized control of DGs and DSTATCOM with communication infrastructure for a micro grid, the reactive compensation and power quality improvement will be successfully done and this is the main contribution of the paper. The reactive compensation will be acted quickly depending upon power flow in the line within the permissible voltage regulation limit by the proposed control. The Stable operation will involve the converter control and data traffic analysis with integrated communication network.

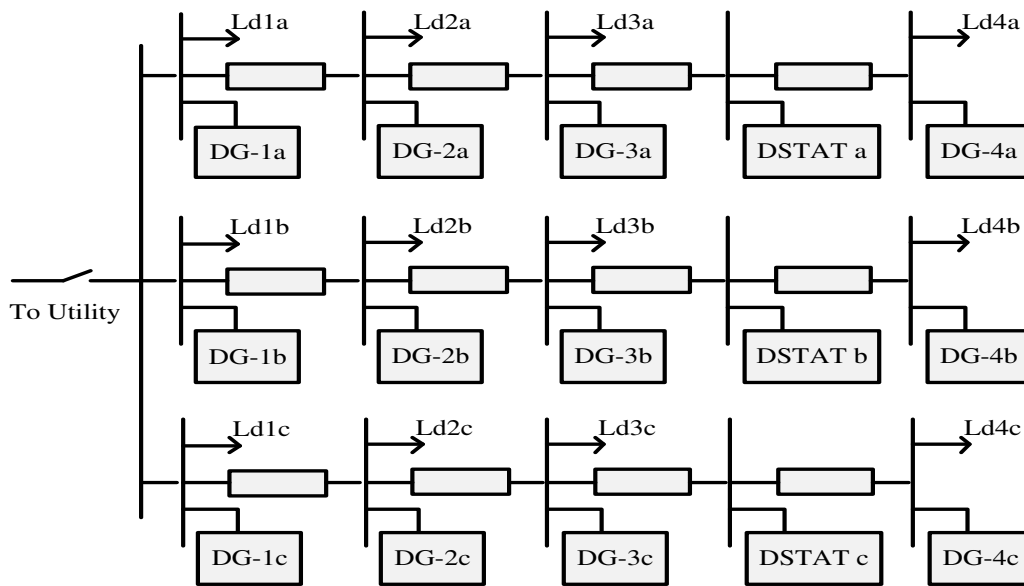


Fig. 1. System under consideration

## 2. Structure of Micro Grid system

The DGs and loads are connected with three feeder sections which form the system under consideration shown in Fig. 1. The first DG attached to phase a as DG1a. The DGs are interfaced with voltage source converters (VSC). The maximum available power and any additional power required by loads will be supplied by DGs and power utilities during the grid connected mode. The total demand in power will be provided by DGs during island operation. Partial load shedding is done to meet the power balance, based on the condition if the power demand in the island mode is more than the total power output of the DGs. Representation of Loads is given by  $Ld1a$ ,  $Ldb1$ , etc. The single phase

compensating devices (DSTATCOM) at various locations are represented as DSTAT a, DSTAT b, and DSTAT c. The impedance of the feeder impedance will be also taken into account. Tables' I-IV shows all the system parameters and DG ratings. Sections II and III show the control techniques of the compensating devices and DGs

**Table-I:** Grid and load in the micro grid

<b>Grid</b>	
Voltage	401 V L-L RMS
Frequency	50 HZ
Line impedance	$R=0.1 \Omega$ , $L=0.001$ H
<b>Load Type</b>	
Resistive	Single phase resistive

### 3. Reactive power compensation improvement by communication and control

Communication and control principle of the DGs and DSTATCOM is described in this section. Depending upon line power flow and line voltage, the regulation of compensation will be done to improve reactive compensation in the proposed method. The active and reactive power flow in feeders will be varied with the voltage due to the frequent switching of load and variable output power of DG in a micro grid. The power flow in the control of DSTATCOM is very profitable to achieve a better and faster control of voltage profile. The following assumptions are being made which are given below.

- a. Based on converter safe operating area, the reactive power generation is limited by the reactive current limit and the maximum available power is brought in by DGs in the micro grid. The active current (d axis) and maximum current rating will involve the reactive current limit.
- b. In islanded mode due to low reactive power demand, the DGs reactive power is shared in proportional to their rating.

- c. DSTATCOM will generate the equivalent amount of reactive power when a maximum reactive power limit is reached by DG and the bus voltage at DG falls below the voltage regulation limit.
- d. Reactive power limit in DG if stays for five cycles then the real power generation in its limit will be lowered by increasing the capability of reactive power.
- e. There will be a limit for possible reactive power generation or absorption by the DSTATCOM. The converter maximum rating and its parameters in the circuit is related to this limitation [4].

The active and reactive power relations are first formed in a two machine example as shown in Fig. 2. Reactive power compensation is later considered in a configuration of multi machine. The DGs and DSTATCOM control principle formation is discussed in these two examples. The consideration of operations of both the grid-connected and islanded modes is taken into account

**Table –II:** Controller and converter parameters

No. of converters in Phase A	4		
No. of converters in Phase B	3		
No. of converters in Phase C	3		
Rated output power of DGs	Phase A	Phase B	Phase C
DG- 1	1.5 KW	4.0 KW	5.0 KW
DG- 2	4.0 KW	4.0 KW	1.5 KW
DG- 3	5.0 KW	3.0 KW	5.0 KW
DG- 4	5.0 KW	xx	xx
Converter structure	Single phase H bridge Inverter		
Converter loss	R= 0.1 $\Omega$ Per phase		
Transformer	0.400/0.230 KV, 0.5 MVA, Ltr=4.4 mh		
LC Filter	Lf = 49.8 mH, Cf= 50 $\mu$ F		

**Table-III:** Gains of DG controller parameters

Power controlled Proportional Gain Kp	0.001
Power controlled Integral Gain Tn	0.01
Reactive power controller Proportional Gain Kq	0.0013
Reactive power controller Integral Gain Tn	0.011
d Axis Current Controller Proportional Gain Kid	2
d Axis Current Controller Integral Gain Tn	0.01
q Axis Current Controller Proportional Gain Kid	2
q Axis Current Controller Integral Gain Tn	0.012
Voltage controller gain m1	0.016 V/Var

$P_{\text{reflim}}$  and  $Q_{\text{reflim}}$  represents the DG-1 maximum available active and reactive power and  $V_{\text{Imag}}$  represents the converter voltage reference of DG-1 which is given by the generation of reference voltage shown in next section. The voltage reference for DG-1 converter is regulated with droop control in islanded mode [25] as

$$V_{\text{lref}} = V_{\text{Imag}} - m_1 Q_1 \quad (1)$$

where  $Q_1$  is limited to maximum reactive power value  $Q_{1\text{max}}$ . Now, the power flow from Bus 1 for system shown in Fig. 2 can be written as

$$P_1 = \eta [R_{D1} (V_{11} - V \cos(\delta_{11} - \delta)) + X_{D1} V \sin(\delta_{11} - \delta)]$$

$$Q_1 = \eta [-R_{D1} V \sin(\delta_{11} - \delta) + X_{D1} (V_{11} - V \cos(\delta_{11} - \delta))]$$

where  $\eta = V_{11}/(R_{D1}^2 + X_{D1}^2)$ .

From the above equation, multiplying  $Q_1$  by  $R_{D1}$  and subtracting the product of the multiplication of  $P_1$  and  $X_{D1}$ , we get

$$X_{D1} P_1 - R_{D1} Q_1 = V_{11} V \sin(\delta_{11} - \delta) \quad (2)$$

In a similar way, we also get

$$R_{D1} P_1 + X_{D1} Q_1 = V_{11}^2 - V V_{11} \cos(\delta_{11} - \delta) \quad (3)$$

The voltage magnitude control of the load and its angle is not associated with the DG-1. Thus, the linearization of (2) and (3) around the nominal values of  $V_{110}$  and  $\delta_{110}$  results in

$$X_{D1} \Delta P_1 - R_{D1} \Delta Q_1 = (V_{110} V) (\Delta \delta_{11} - \Delta \delta) + (\delta_{110} V) \Delta V_{11} \quad (4)$$

$$R_{D1} \Delta P_1 + X_{D1} \Delta Q_1 = (2V_{110} - V) \Delta V_{11} \quad (5)$$

where  $\Delta$  indicates the perturbed value. From (4) and (5), the output voltage magnitude and angle of a DG-1 can be written in terms of real and reactive power as

$$\begin{aligned} \begin{bmatrix} \Delta \delta_{11} - \Delta \delta \\ \Delta V_{11} \end{bmatrix} &= \mathbf{K}(\mathbf{V}) \begin{bmatrix} \frac{X_{D1}}{Z_1} & \frac{-R_{D1}}{Z_1} \\ \frac{X_{D1}}{Z_1} & \frac{R_{D1}}{Z_1} \end{bmatrix} \begin{bmatrix} \Delta P_1 \\ \Delta Q_1 \end{bmatrix} \\ &= \mathbf{K}(\mathbf{V}) \mathbf{T} \begin{bmatrix} \Delta P_1 \\ \Delta Q_1 \end{bmatrix} \end{aligned} \quad (6)$$

Where the impedance  $Z_1$  and the matrix  $\mathbf{K}(\mathbf{V})$  are given by

$$Z_1 = \sqrt{R_{D1}^2 + X_{D1}^2}$$

$$\mathbf{K}(\mathbf{V}) = Z_1 \begin{bmatrix} V_{110} V & \delta_{110} V \\ 0 & 2V_{110} - V \end{bmatrix}^{-1}$$

Thus, the change in voltage of Bus 1 can be written in terms of change in power flow as given in (5). If we need to provide reactive compensation at the load point in Fig. 2, it would be beneficial to consider the change in real and reactive power flow at Bus 1 due to change in voltage  $V$ . Linearizing (4) around the nominal voltage  $V_0$ , we get

$$R_{D1} \Delta P_1 + X_{D1} \Delta Q_1 = -V_{11} V_0 \Delta V$$

$$\Delta V = -\frac{R_{D1} \Delta P_1 + X_{D1} \Delta Q_1}{V_{11} V_0} \quad (7)$$

Thus the power change is related to changes in load and the load voltage will change according to the reactive power injection at load point as shown in (7). The reference voltage of the DSTATCOM is then derived as

$$V_{\text{statref}} = V_0 - m_{\text{STAT}} Q_{\text{STAT}} +$$

$$K_1 \frac{R_{D1} P_1 + X_{D1} Q_1}{V_{11} V_0} + K_2 \frac{R_{D2} P_2 + X_{D2} Q_2}{V_{22} V_0} \quad (8)$$

Where  $Q_{\text{STAT}}$  represents the available maximum capacity,  $Q_{\text{STATLIM}}$  represents limited capacity of DSTATCOM, and  $m_{\text{STAT}}$  represents the gains. The reference voltage of DSTATCOM always kept within permissible voltage regulation limits by choosing the values of  $K_1$ , and  $K_2$  with maximum real and reactive power flow. Two control loops are involved in the proposed method of control. The first two terms in (8) indicate the primary control loop based on the local measurements, while the secondary control loop is based on the voltages and power flow in the line. The next section shows the DSTATCOM converter control in detail. The arrangement of the multi machine is shown in Fig. 3. Four buses have four DGs connected to it and the Bus DSTAT has one DSTATCOM connected to it.  $P_{ii}, Q_{ii}$  represents the generation of active and reactive power and  $P_{Li}, Q_{Li}$  represents the power demand in load at each bus.  $P_i, Q_i$  represents the power flow at each bus. Similar to (8), the voltage reference for DSTATCOM is derived as

$$V_{\text{statref}} = V_0 - m_{\text{STAT}} Q_{\text{STAT}} + K_1 \frac{R_{D1} P_1 + X_{D1} Q_1}{V_{11} V_{22}} + K_2 \frac{R_{D2} P_2 + X_{D2} Q_2}{V_{22} V_{33}} + K_3 \frac{R_{D3} P_3 + X_{D3} Q_3}{V_{33} V_{\text{stat}}} + K_4 \frac{R_{D4} P_4 + X_{D4} Q_4}{V_{44} V_{\text{stat}}} \quad (9)$$



The feeder at the far end has more drops in voltage and the reactive current limit is reached earlier by the DGs at the far end. Based on the current rating, reactive power generation will be in small amount supplied by the DGs near to the utility connection. The voltage at any location will fall below the permissible voltage regulation limit in autonomous mode. The DGs which are close to DSTATCOM will run in proportional to slope of reactive power within voltage regulation and the DGs which are far to DSTATCOM with the operation of DSTATCOM on either side may reach their reactive power limit. The injection of more amount of reactive power is not possible by a DG if it reaches the reactive power limit. The voltage of the buses of DSTATCOM and adjacent DSTATCOM will be improved by the injection of reactive power. The location of feeder however will not be influenced by it far from them. The increase in injection of the reactive power of DG will give

rise to increase in improvement of voltage nearby. The reactive current limit of the converter must be increased in order to increase the injection of reactive power above the reactive power limit and this is possible only by lowering the generation of active power within a limit based on the bus voltage as

$$P_{\text{ref}} = P_{\text{maxavail}} - \lim [0, 0.05 \text{ pu}, k_{\text{pr}} (V_{110} - V_{11})] \quad \text{if } (V_{110} > V_{11}) \quad (10)$$

Where the RMS value of nominal bus voltage is indicated by  $V_{110}$  and the RMS value of actual voltage is indicated by  $V_{11}$ . The reference power reduction stays within permissible limits with minimum voltage and gain  $k_{\text{pr}}$ . Under voltage condition is effective only when this is limited to positive error.

**Table –IV:** Gains of DSTATCOM controller parameters

Power controller Proportional Gain $K_p$ s	0.0013
Power controller Integral Gain $T_{ns}$	0.012
Reactive power controller Proportional Gain $K_q$ s	0.0034
Reactive power controller Integral Gain $T_{ns}$	0.04
d Axis Current Controller Proportional Gain $K_{id}$	2.5
d Axis Current Controller Integral Gain $T_n$	0.016
q Axis Current Controller Proportional Gain $K_{iq}$	2
q Axis Current Controller Integral Gain $T_n$	0.012
Voltage controller gain $m$ STAT	0.012 V/Var

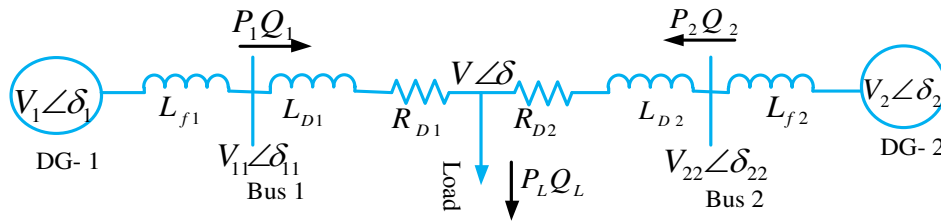


Fig. 2. Two machine system

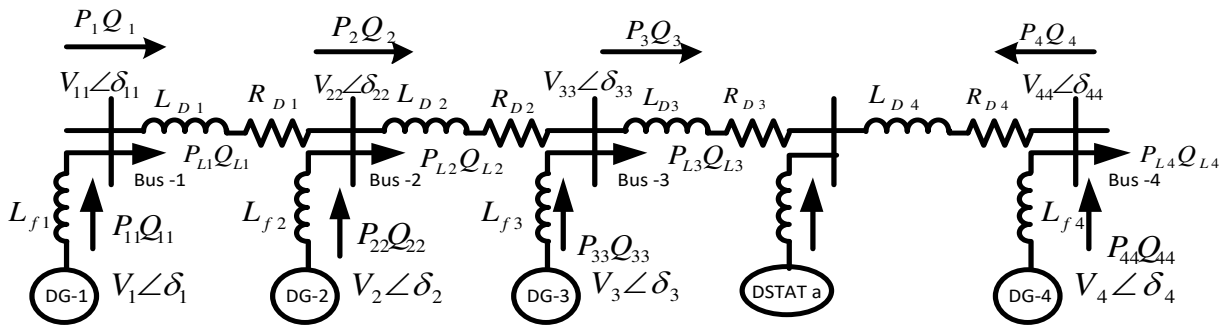


Fig. 3. Multi machine system

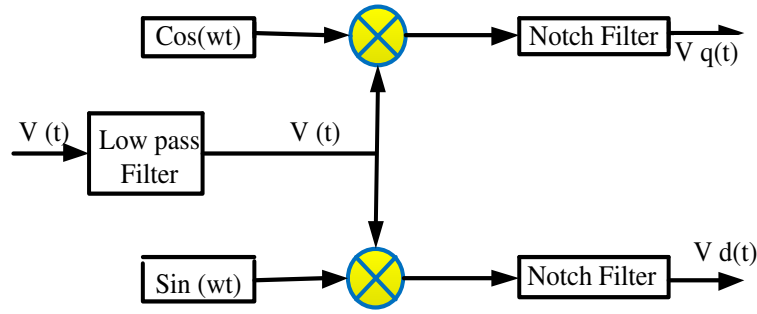


Fig. 4. Single phase DQ transformation

The reactive current reference is then calculated as

$$i_{\text{reactivelimit}} = \sqrt{(i_{\text{max}}^2 - i_d^2)} \quad (11)$$

where,  $i_{\text{max}}$  represents the rating of maximum current in converter current rating and  $i_d$  represents the active power current of converter at d axis. The voltage at local bus and this limit of new reactive current involves the generation of reference of reactive power. The low voltage buses more relaxation of reactive current limit as observed from (10). The reduction in generation of active power is minimal when the voltage closes to minimal values.

#### 4. DSTATCOM and DG'S converter control operation

The structure of the converter and control of DG and DSTATCOM is described in this section. A technique of transformation for single phase is explained by DQ transformation in three phases. The transformation of current and voltage in DSTATCOM and DG is done by using the same technique. Fig. 4 shows the implementation of the transformation of current and voltage. The harmonics at switching frequency are first eliminated by the low pass filter, a product of  $\sin(\omega t)$  and another by  $\cos(\omega t)$  and finally then to increase the frequency of line twice a notch filter is used in order to cancel the terms of this frequency that appeared due to the previous stage. A phase-locked loop will give a precise synchronization.

$$V(t) = V_m \sin(\omega t - \Phi)$$

$$V(t) = V_d \sin(\omega t) - V_q \sin(\omega t)$$

Where,  $V_d(t) = V_m \cos(\Phi)$  and

$$V_q(t) = V_m \sin(\Phi).$$

#### A. DG

The control and structure of all the converters of DGs are same. Description of Control and the structure of the converter of Only DG-1 are done here. The structure of the converter for DG-1 is shown in Fig. 5. Four IGBT switches are required for forming the single phase converter and the output as side voltage  $e$  of the converter is connected through the transformer to the output filter capacitor ( $C_f$ ) as shown in Fig. 5.  $R_{tr}$  and  $L_{tr}$  represent the transformer loss and inductance. The PCC will have the DG is connected to it through output inductance  $L_f$ . Table II shows the data of the converter. DG-1 has the scheme of control of the converter shown in Fig. 6. The control of frequency due to generation of reference voltage is shown in Fig. 6. Depending on the converter current limit, the generation of active and reactive power is done and is shown in Fig. 7 and its current loop is shown in Fig. 8. The island mode of operation involves active regulation of frequency and voltage and is shown by last block in Fig. 6. The voltage angle and its magnitude are controlled by active power output [25] and regulation of reactive power as shown in (1). The voltage reference calculation block will generate a reference voltage which is directly fed to the converter in a grid-connected mode. With the help of communication network shown, the measured power and voltage are communicated to DSTATCOM. Based on current limit and power available, the power reference generation block shown in Fig. 7 will generate the reference active and reactive power. The measured and reference power will generate the reference current as shown in Fig. 8. The d and q axis reference currents are calculated by using the error in active power and reactive power. The generation of reference voltage of the converter is shown in Fig. 9. The current errors are passed through the PI controller and added to the d-q axis voltage reference as shown in Fig. 9.

## B. DSTATCOM

The DSTATCOM has the structure of the converter is shown in Fig. 10. Table IV shows the parameters of DSTATCOM. The H Bridge has the DC side capacitor connected to it. The output of filter capacitor at the AC side voltage  $e_{stat}$  is connected through a transformer.  $i_{STAT}$  and  $V_{stat}$  represents the DSTATCOM output current and voltage. DSTATCOM has the converter control scheme shown in Fig. 11. The reference output voltage of DSTATCOM is represented as  $V_{statref}$  and is given in (9). The fixed value of DC voltage is represented as  $V_{cref}$ . The generation of reference is shown in Fig. 12. The generation of d and q axis reference currents is obtained by using error in dc capacitor voltage through a PI controller and error in DSTATCOM output voltage as shown in Fig. 12. The DGs and DSTATCOM have the methods of control which are shown in Fig. 13. The maximum available power will be supplied by the DG in grid-connected mode. The island mode will have the activation of regulations of droop voltage and frequency. The reference of active power will be

changed according to (10) when the reactive power limit is reached by DG. The operation of DSTATCOM op using both communicated and local measurements is described in (9). The strategy of control has the overview diagram is shown in Fig. 14. The other DGs have the same control strategies just like DG-1. The communication network will provide the power flow and voltage of the DG buses by DSTATCOM as shown. The reactive compensation usually involves the feeder having a single DSTATCOM at the far end. Installation of Multiple DSTATCOM must involve control of voltage and power flow based on the diffusion of DG in the micro grid. Multiple DSTATCOM arrangements will have modified. control strategies. The feeder can be divided in one way for reactive compensation in different zones where each DSTATCOM takes care of its own zone. The DSTATCOM will have communication with the DGs in that zone. The improvement of voltage profile and control of the zone will be done by communication of DSTATCOMs with each other

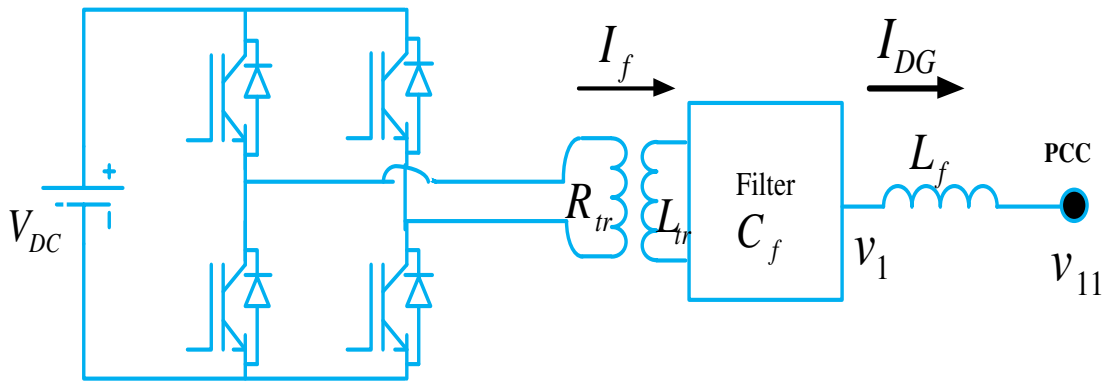


Fig. 5. DG-1 Converter structure

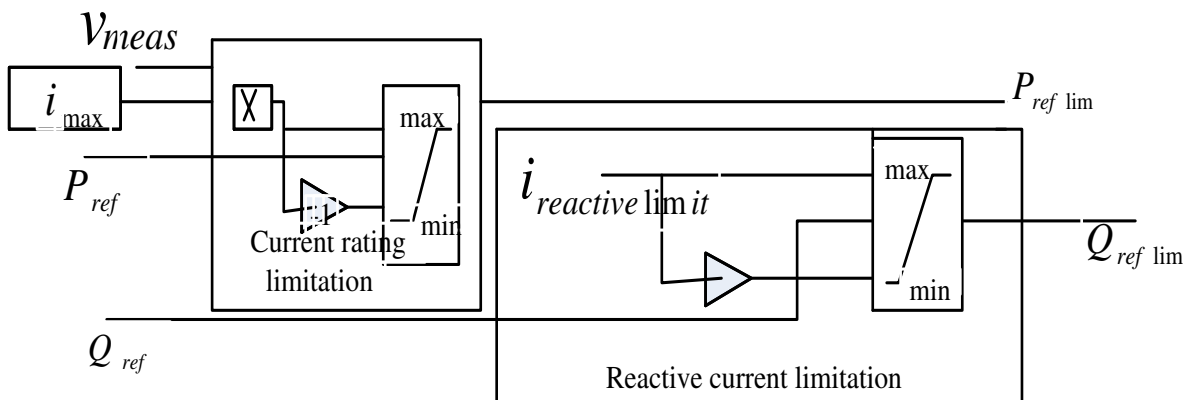


Fig. 7. Reference power generation



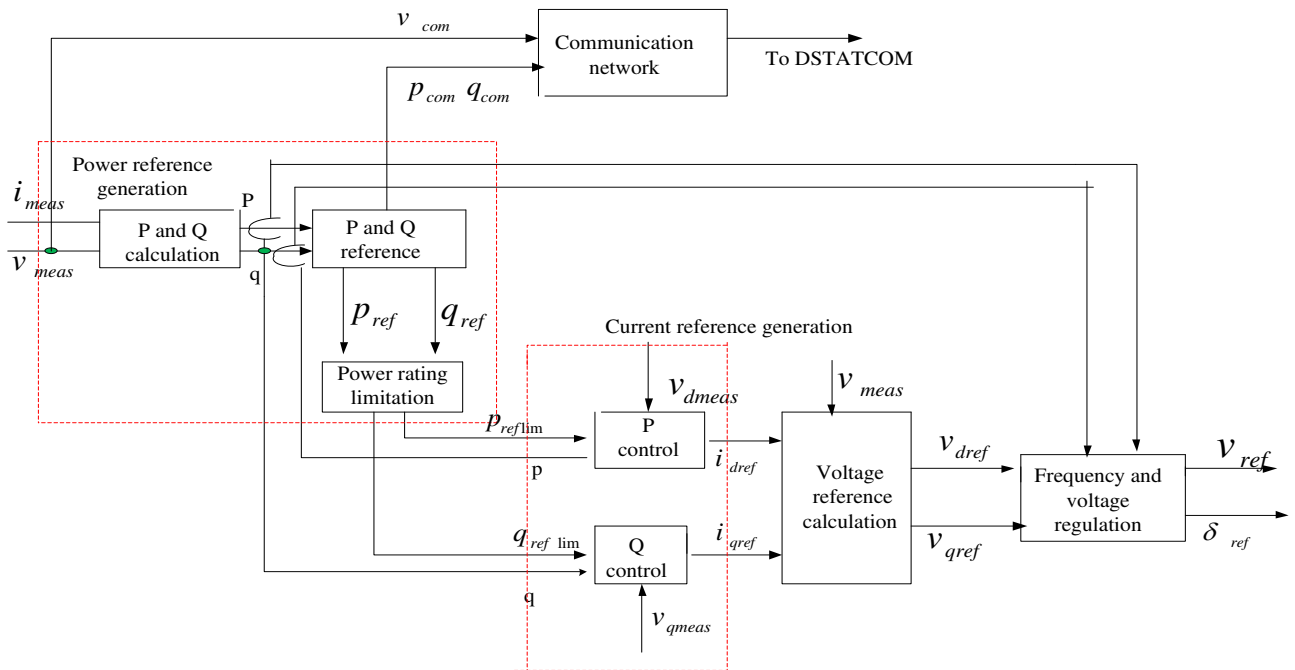


Fig. 6. DG-1 Converter control

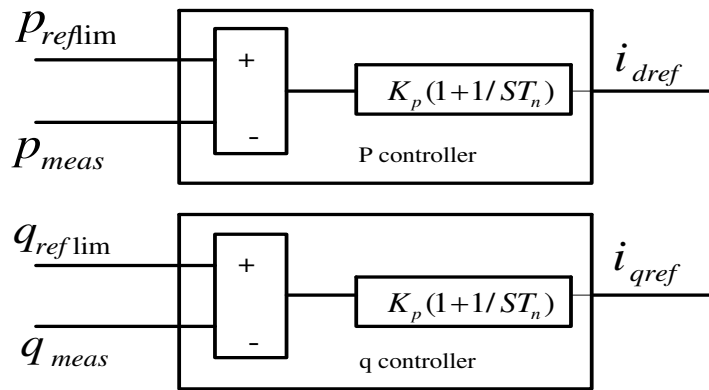


Fig. 8. Reference current generation

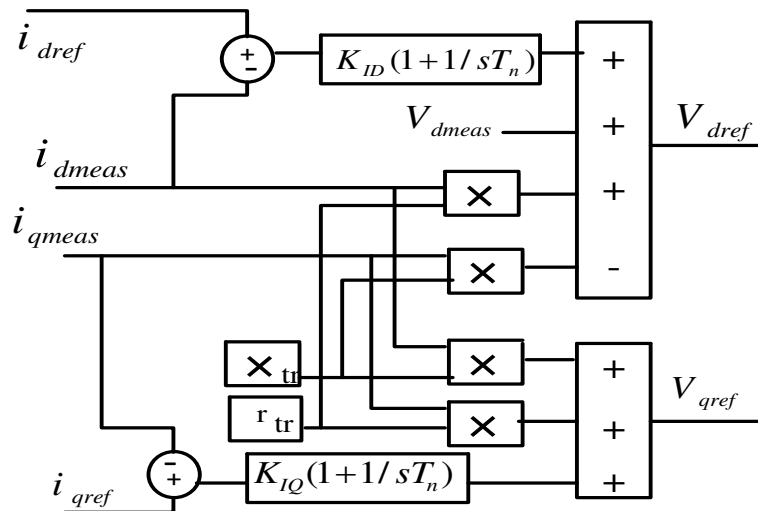


Fig. 9. Reference voltage generation

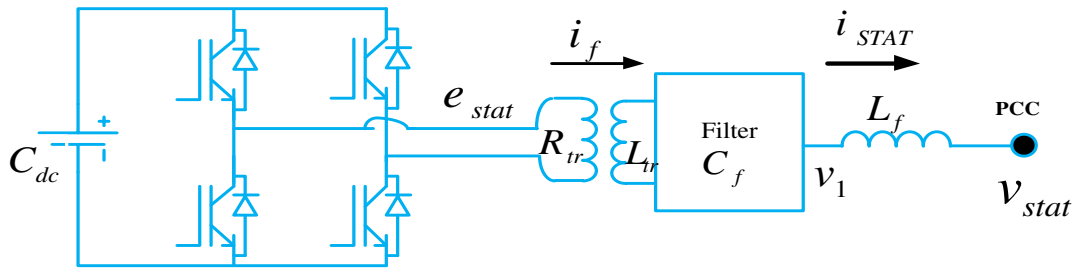


Fig. 10. Converter structure of DSTATCOM

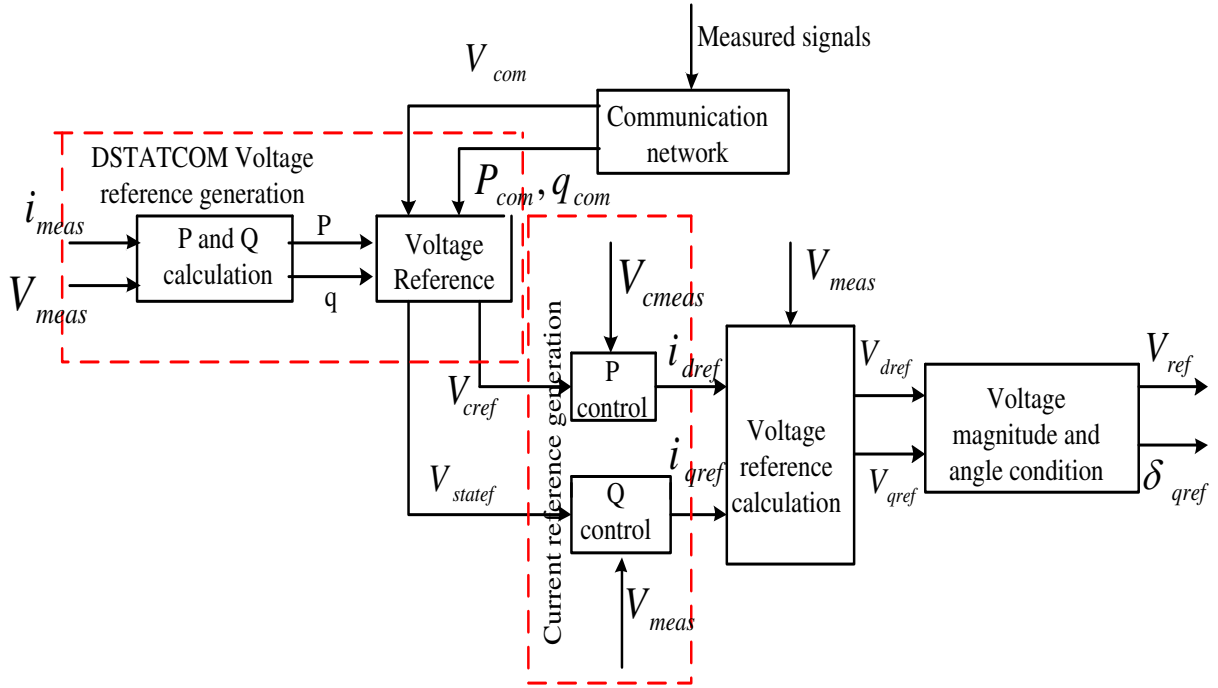


Fig. 11. Converter control scheme for DSTATCOM

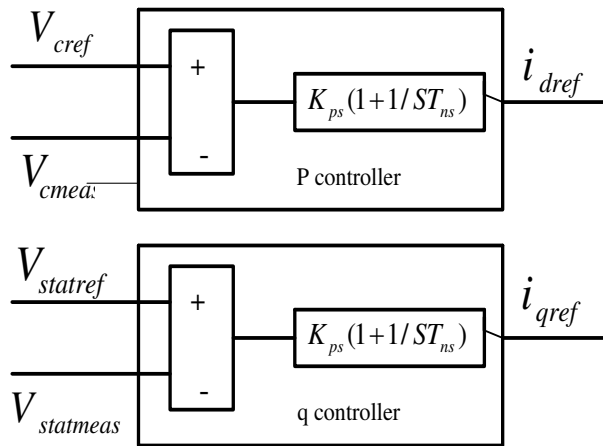


Fig. 12. Converter reference current generation

## 5. Communication network information transfer study

The study, performance analysis and limitations of the communication scheme are described in this

section. The implementation of communication network is done by using Qualnet [26] as shown in Fig. 15. The simulation of communication networks in wired and wireless packet mode is done by using a network simulation tool called Qualnet. The

communication between DGs and DSTATCOM is indicated by green lines and the dark, thick lines show the geographical spans of the phases. Phase A has four single-phase DGs, Phase B has three single phase DGs and Phase C has single-phase DG as mentioned earlier as shown in Fig. 15. DSTAT-a, DSTAT-b, and DSTAT-c represents the DSTATCOM in single-phase operation as shown in Fig. 15. The DSTATCOMs and the DGs will have the network communication of low bandwidth between them. Table V shows the parameters of the Communication network. Communication of DSTATCOM along the different phases having flow of real power and reactive power is done. The total data packet will be sent from each communication node with the help of network communication as shown in Fig. 15 and Fig. 16, the packet of total data received by each communication node as shown in Fig. 17

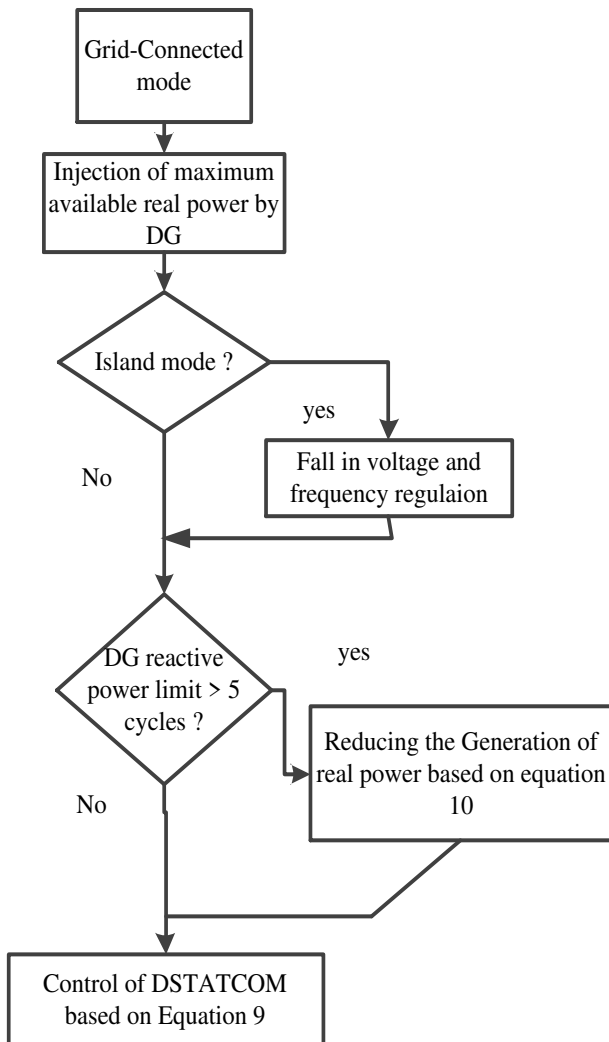


Fig. 13. Control methods

The positions of DSTATCOM are represented by

nodes 1, 2, and 3. The delay of end-end is shown in Fig. 18. The delay of end to end is within 1.5 ms is observed.

**Communication Bandwidth:** The delay of end to end is influenced by communication bandwidth. Consideration of communication of a 10 MB/s is described in Fig. 18. Consideration of phase a 1 MB/s, in phase b 100 kB/s, and in phase c 10 KB/s bandwidth is done to analyze and shows the influence on bandwidth. The delay of end to end is shown in Fig. 19. 20 ms (phase a), 0.1 s (phase b), and 1.0 s (phase c) are varied and controlling of main frequency is done by having a bandwidth more than 100 KB/s. The essential requirement will give an exact choice of bandwidth. The data packets received by each communication node will be same as shown in Fig. 20. All the phases receive the same number of data packets from communication node.

**Table - V:** Communication Network parameters

Number of Nodes	16
Link Type	Wired
MAC Protocol	Abstract MAC Link
Bandwidth	100 kbps
Link propagation delay	1 ms
Header Size	224 bits

**Communication Failure:** The DSTATCOM works only with primary control based on local measurement in case of a communication failure. The information about power flow before node 15 is not communicated to DSTAT-a due to failure of node 15 (DG-3a) which lead to the investigation of the impact of node failure. The communication nodes will have total packets of data received as shown in Fig. 21. The control of secondary loop will have less accuracy and more packet loss due to node failures. The primary control loop is used for the phase based on local measurements in case of a node failure in DSTATCOM location (node 1, node 2, or node 3). The communication node 1 will have the total packets of data received as shown in Fig. 22. The primary control loop has operation of DSTAT-a as no information is communicated to node 1.

## 6. Simulation of power and communication network in a closed-loop

The simulation of the power network and communication network in a closed-loop is described in this section. By using SIMPOWER and TRUETIME, the power network and communication

network are simulated. The MATLAB Platform in SIMULINK as shown in Fig. 23. The different situations in test system shown in Fig. 1 as follows

- Situation 1: Reactive compensation is not included
- Situation 2: Local measurement, including reactive compensation.
- Situation 3: Proposed method involving reactive compensation.
- Situation 4: DG has the failure of communication node.
- Situation 5: DSTATCOM has the failure of communication node.
- Consideration of a similar set of change in output power of DG and sequence of switching

the load is done to compare the controller performance for all the situations. The effectiveness of the proposed method is tested by three different series of phenomenon. Series-1, Series-2, and Series-3

Represents the three testing series

- **Series-1:** Operation in a grid-connected mode.
- **Series-2:** Operation in an autonomous mode.
- **Series-3:** Operation in grid-connected followed by islanding mode.

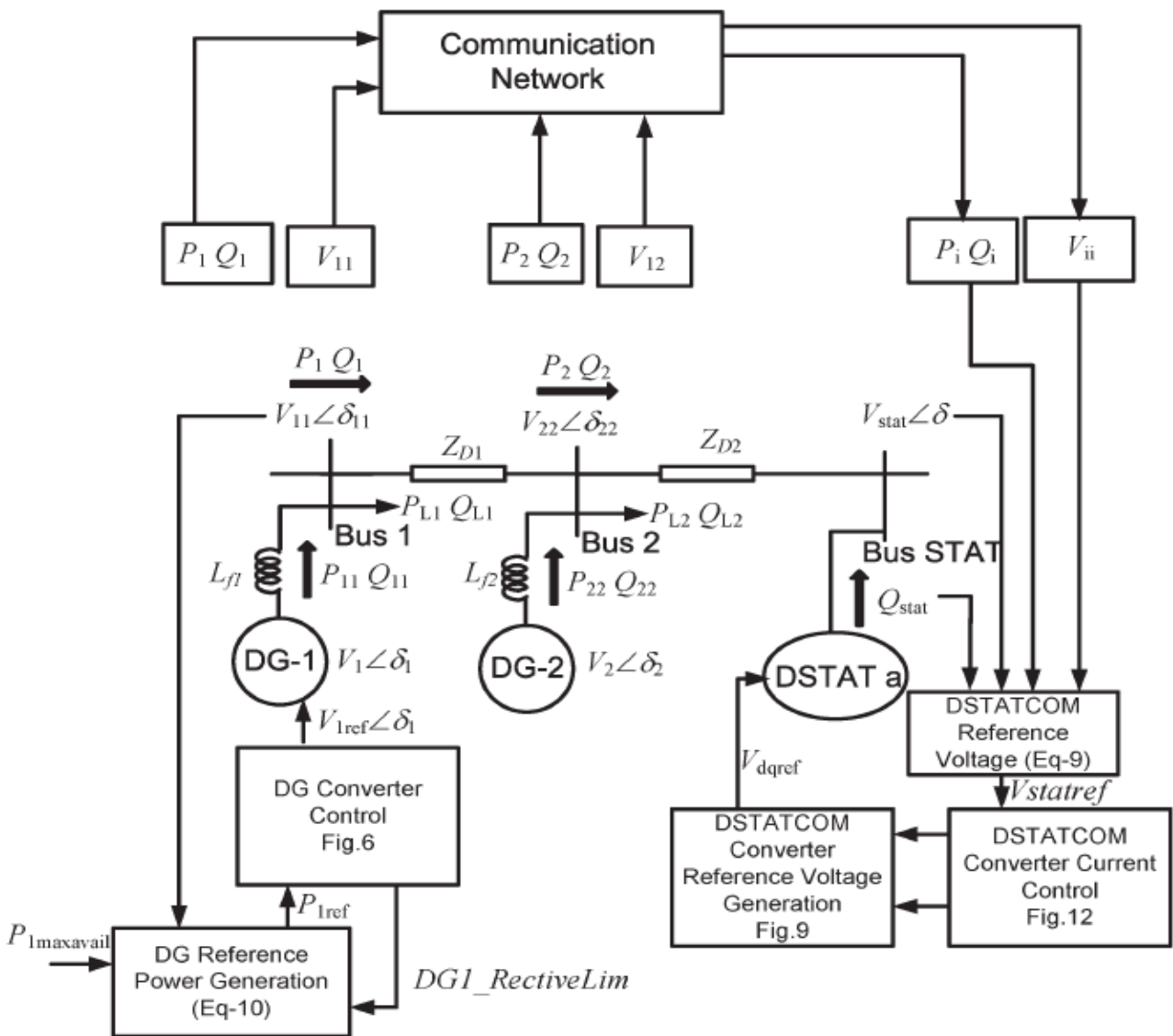


Fig. 14. Control overview of the scheme

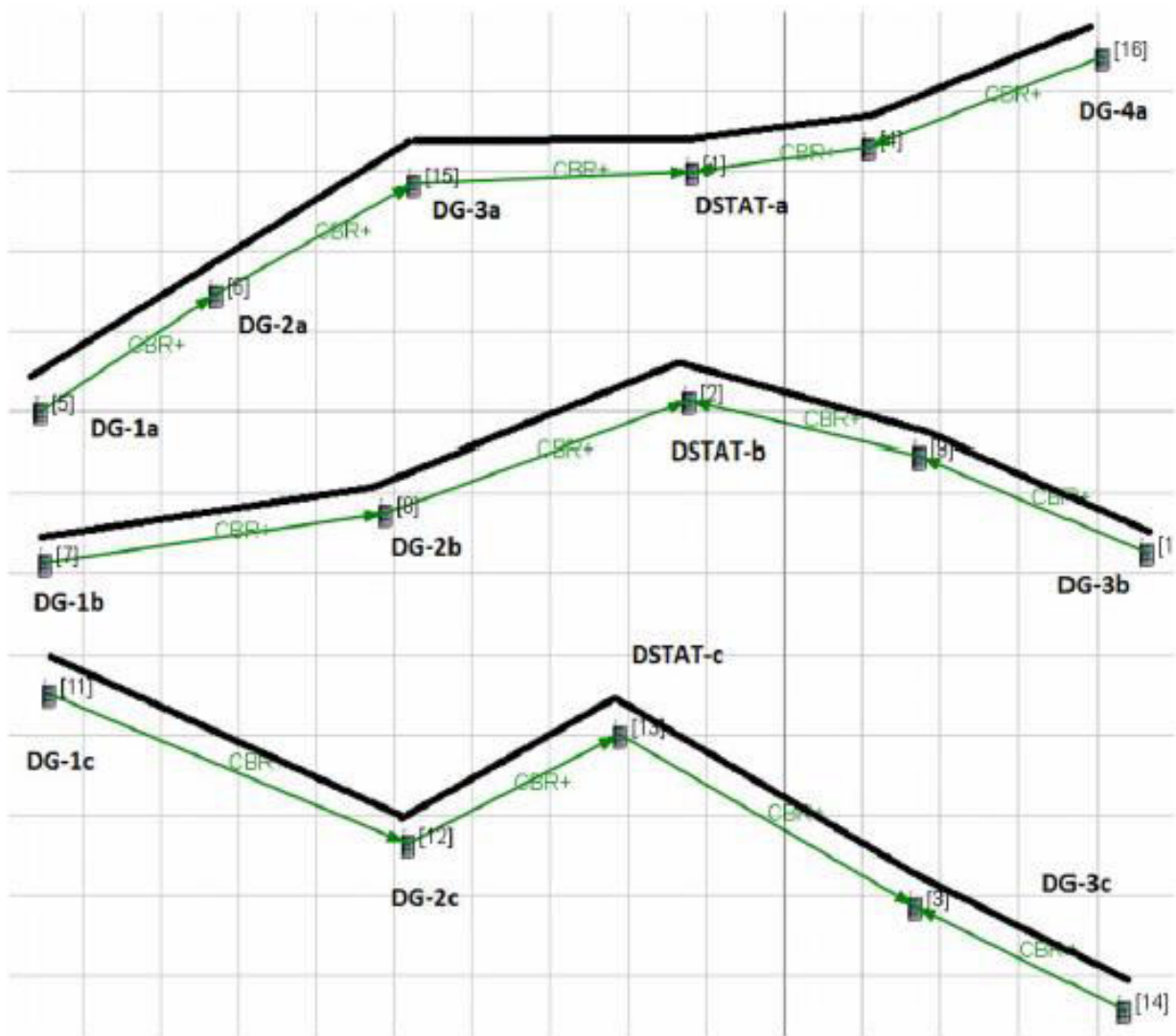


Fig. 15. Communication network

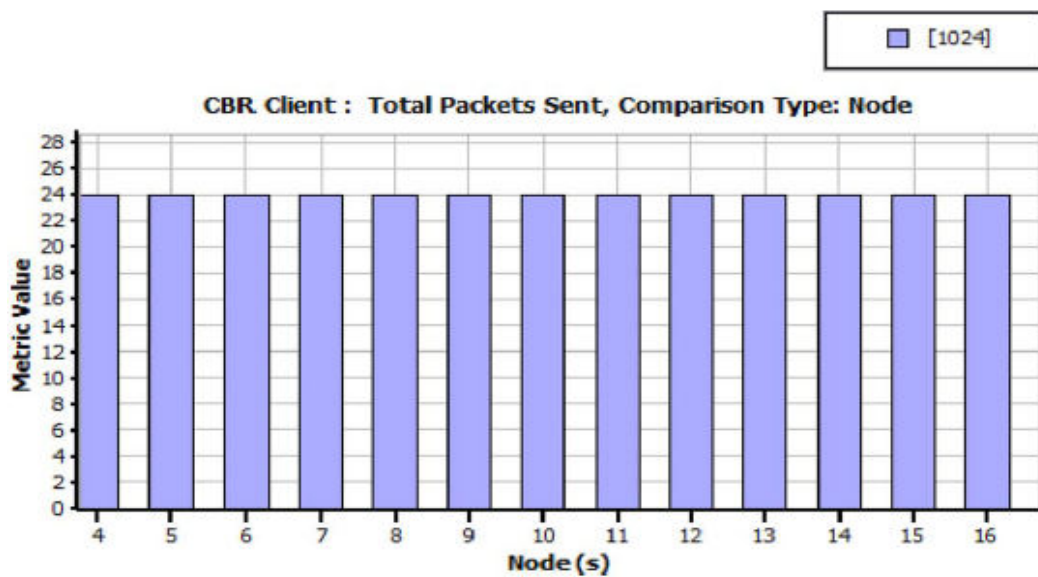


Fig. 16. Packets of total data sent



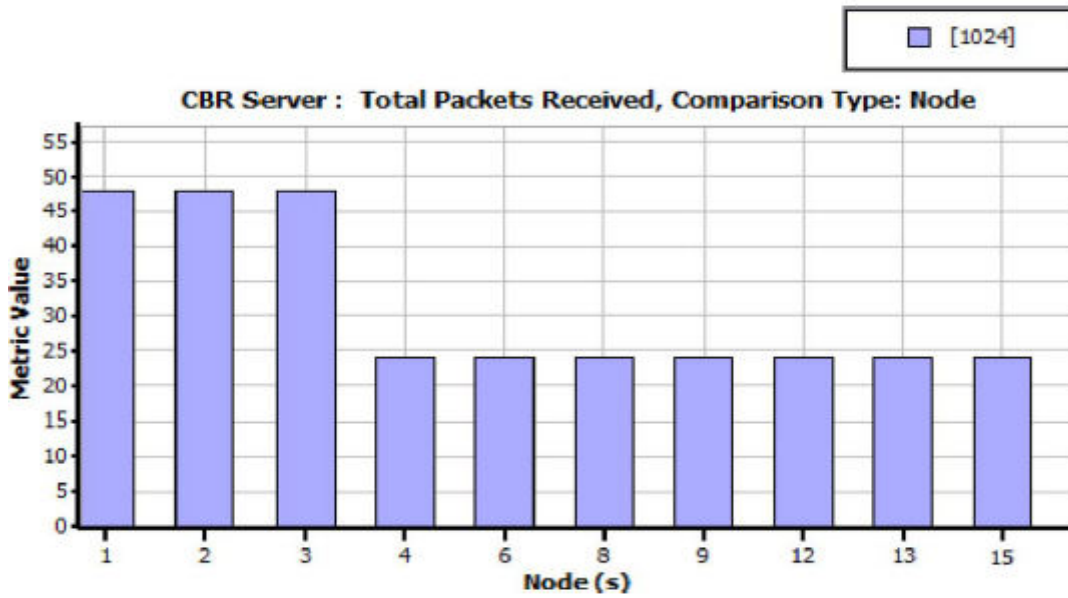


Fig. 17. Packets of total data received

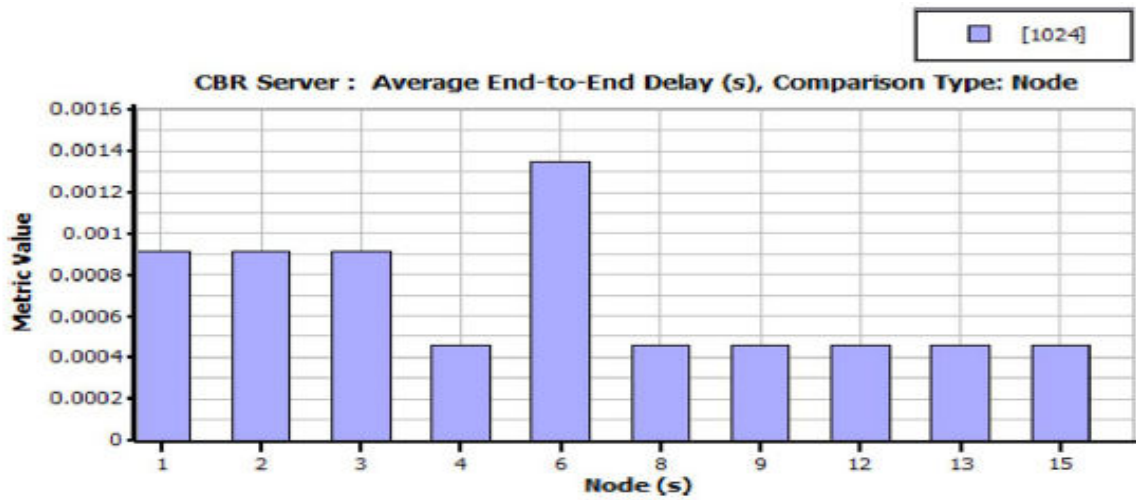


Fig. 18. 10 MB/s delay end to end

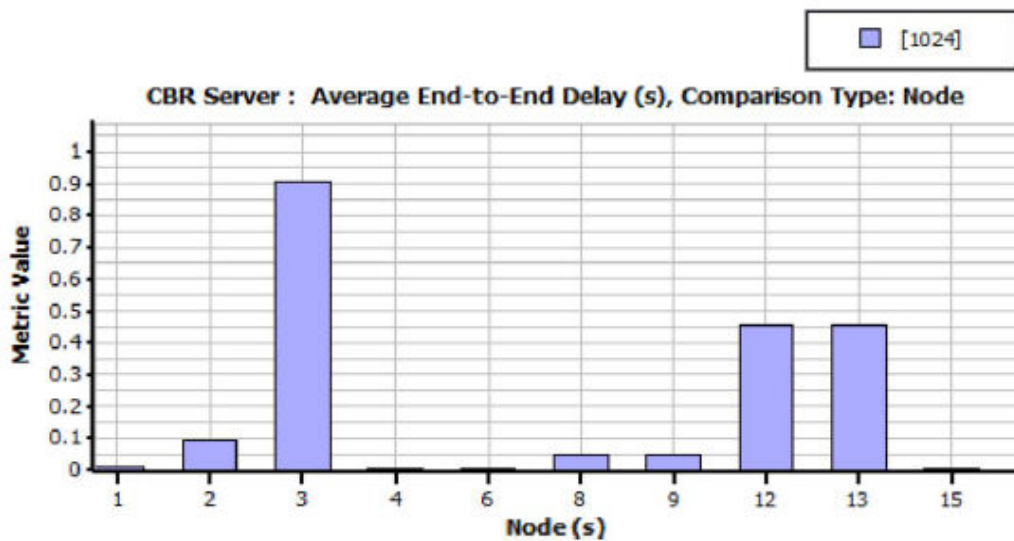


Fig. 19. End-to-end delay phase a – 1 MB/s, phase b 100 kB/s, and phase c 10 kB/s

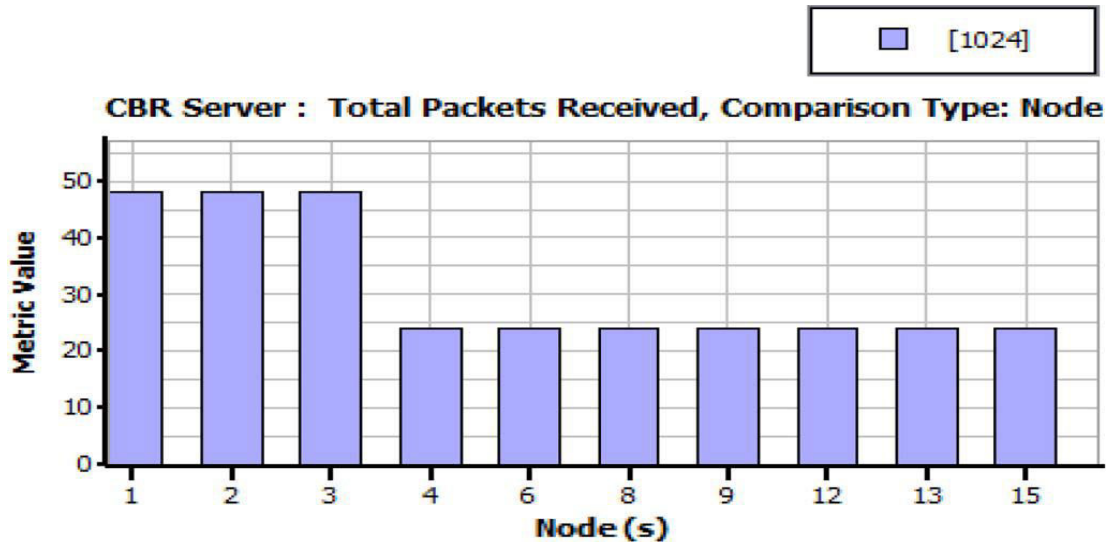


Fig. 20. Total packet received with phase a -1 mb/s, phase b 100 kb/s, and phase c 10 kb/s.

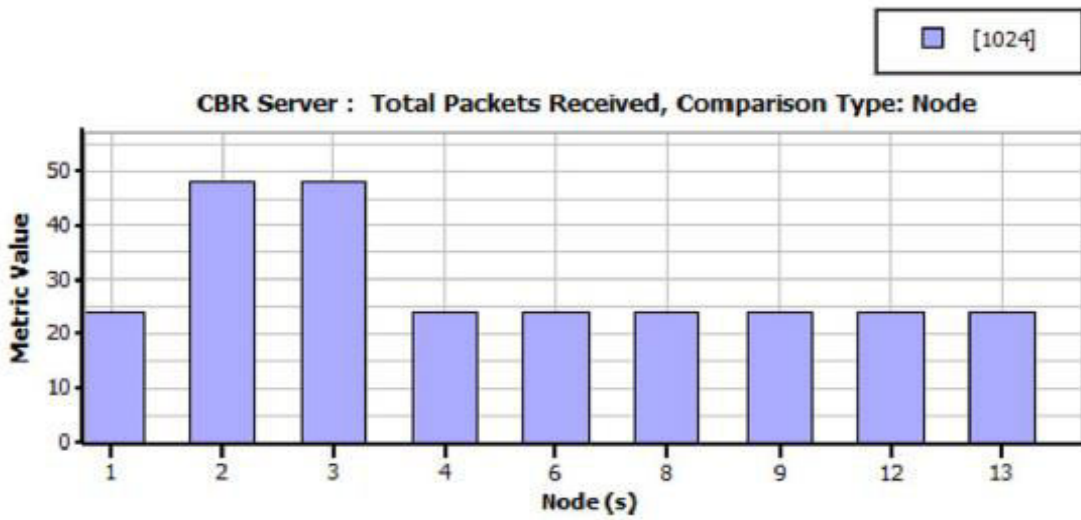


Fig. 21. Packets of data received with failure of NODE 15

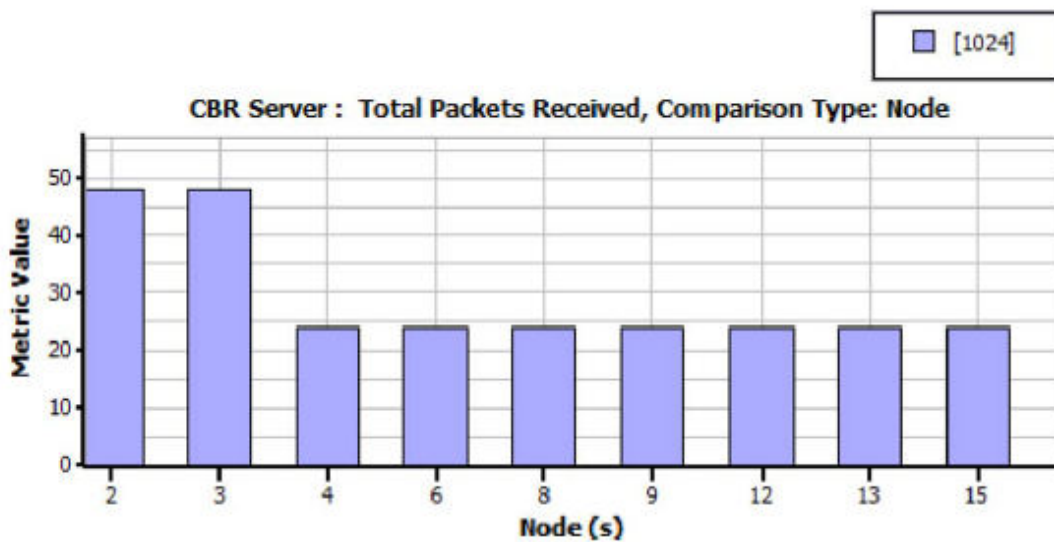


Fig. 22. Packets of data received with failure of NODE 1

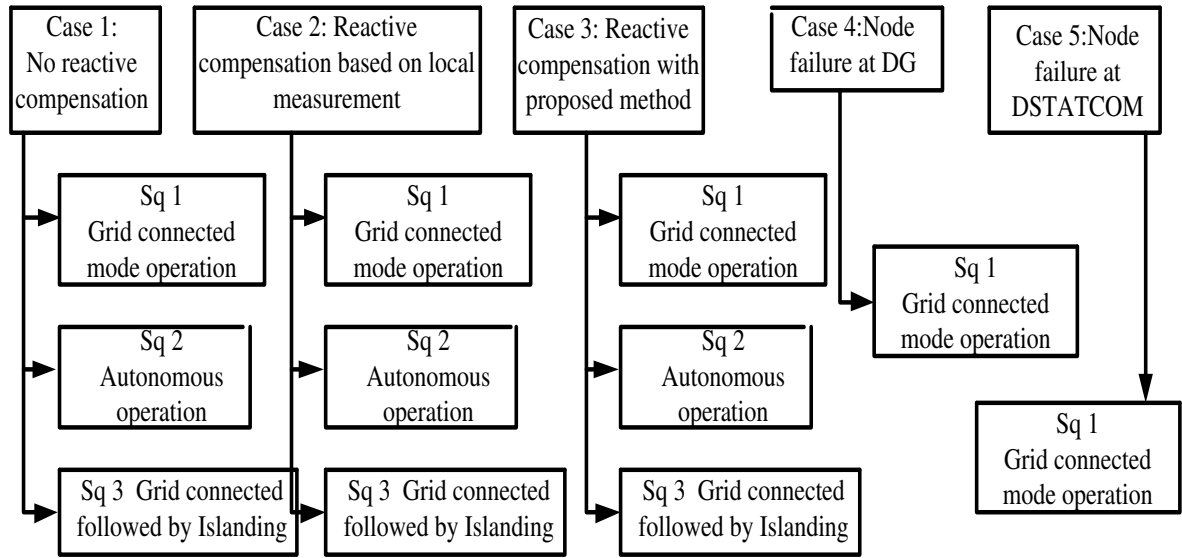


Fig. 24. Simulation layout

**Table-VI:** Simulation results showing rms voltages of phase A

Case	Description	Sq/ Figure	Initial value (V)	In Step1 (V)	In Step2 (V)	Final value (V)
Case 1	No reactive compensation	Sq1- Fig 26(a) Grid connected	Ut.S =234 MF=211 FE=200	N/A	N/A	Ut.S =223.5 MF=189 FE=183
Case 1	No reactive compensation	Sq2- Fig 27(a) autonomous	Ut.S =215.5 MF=212.7 FE=200.3	N/A	V	Ut.S =210.8 MF=207.1 FE=200.2
Case 2	Reactive compensation on local measurement	Sq1- Fig 28 Grid connected	Ut.S =217.1 MF=218.4 FE=217.4	N/A	N/A	Ut.S =221.2 MF=203.4 FE=196.8
Case 2	Reactive compensation on local measurement	Sq2- Fig 29 autonomous	Ut.S =219.8 MF=220.0 FE=208.2	N/A	N/A	Ut.S =218.8 MF=216.5 FE=213.6
Case 2	Reactive compensation on local measurement	Sq-3 Fig 30(a) Islanding	Ut.S =227.2 MF=215.3	Ut.S=216.7 MF=217.2	Ut.S=214.6 MF=213.9	Ut.S =227.7 MF=215.4

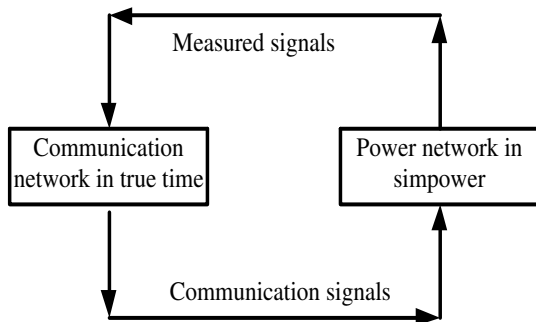


Fig. 23. Simulation of communication network and power network in a closed loop

The information for the three testing series is given below

**Series-1:** Operation of utility connected mode is described in this system. The steady state operation of DGs will have the rated power to which the loads are connected and the phase a, (DG-1a, DG-2a, and DG-3a) have the power output of three DGs connected to it which are limited to 2 kW each. The limitation of reactive power is done to 300 VAR.

**Series-2:** The operation of islanding mode is described in this system. The steady state operation of DGs will have the rated power to which the loads are connected and the three DGs connected at Bus 2 of all three phases (DG a2, DGb2, and DG c2) will have a power output limited to 2 kW each. The limitation of reactive power is done to 400 VAR.

**Series-3:** The operation of utility connected mode is described in this system. The steady state operation of DGs will have the rated power to which all the loads are connected and the islanding operation of the micro grid has taken place at 0.8 s. The demand in load will be supplied by DGs. DG-2a, DG-2b, and DG-2c will have the power output which is limited to 2 kW at 1.1 s. The loads connected at Bus 1 of the phase A and phase B (*Ld1a* and *Ld1b*) are disconnected at 2.0 s to decrease the demand in power in the micro grid. The different series described above are used in each test situation. The layout of simulation is given in detail as shown in Fig. 24. The following sections show the results of simulation obtained at each situation. Table VI shows the initial, intermediate, and final steady-state values of phase A.

**A. Situation 1: Reactive compensation is not included:** Reactive compensation is not included in this situation and the DGs and utility (in grid connected mode) or only by the DGs (in autonomous mode) will; have to supply the total reactive power. The power output of the DGs connected to phase A and three phase voltage profile for series-1 are shown in Fig. 25 and Fig. 26. The problem of voltage regulation is more in the far end compared to feeders in the middle. The utility connected side will have the voltage sag limited within 2%. Series-2 and Series-3 will have the voltage unbalance and RMS voltage which are shown in Fig. 27. The drop in voltage is far more than permissible values which lead to problems in voltage regulation.

**B. Situation 2: Local measurement, including reactive compensation:** The operation of DSTATCOM in a conventional way is described in this situation. The local bus voltage of the DSTATCOM is considered for the injection of reactive power. Series-1 has the RMS voltage as shown in Fig. 28. The injections of reactive power by the DSTATCOMs are shown in Fig. 29. Series-2 and Series-3 have the RMS voltages which are shown in Figs. 30. The improvement of voltage profile is observed compared to the situation where the reactive compensation is not included. In some situations the voltages are below the limit and the operation of reactive power compensation is observed well when very close to DSTATCOM.

**C. Situation 3: Proposed method involving reactive compensation:** The compensation of reactive compensation is described by (9) – (11) where, 1)

The modulation of voltage bus at local loads and the power flow in the line can be done by compensation of reactive power by using DSTATCOM. 2) Range in the injection of reactive power is increased by modulating the injection of DGs real power depending on the voltage sag. The phase A having RMS voltages in Series-1 are described in Fig. 31 (a). The profile in the improvement of voltage is observed within 10% tolerance with the proposed method. Fig. 31(b) shows the injection of in phase A by using DSTAT-a and DGs. DG3a and DG4a reactive power change and validation is described by (10). Series-2 has the response of the system with the controller described in Fig. 32. The well organized and system with stable operation in phase A involves injection of reactive power and voltage from different DSTATCOM. Phase A voltages in series-3 are described in Fig. 33. The observation of voltages within the permissible limits by compensation of reactive power is achieved successfully by using the proposed method.

**D. Situation 4: DG has the failure of communication node:** DG-1a describes the failure of communication node in this situation. The operation of system is performed in series-1 by the proposed method of control. The response of the system is described in Fig. 34. Series-1 describes the change of voltage in the phase A at 1.1 s with a range of limit of power of DG. Simulation of failure of communication node failure is done at 1.75 s and observation in the fall of voltages at utility side is seen. No visibility changes occur in the feeder voltages at the middle and far end.

**E. Situation 5: DSTATCOM has the failure of communication node:** DSTATCOM describes the failure of communication node in this situation. DSTAT-a describes the response of system to a failure of communication node as shown in Fig. 35. Series-1 describes the DG power limit at 1.1s and the operation of system with the proposed controller. The simulation of failure of communication node is done at 1.75 s and observation of feeders having fall of voltages in utility side, middle, and far end are seen. Failure of communication node make DSTAT-a operate just like situation 2 with the confined measurements. The improvements in the voltages are compared to situation 2 by modulating the real power of DG as shown in (10). Regulation of voltage within the permissible limits is achievable in all situations with the proposed controller is shown in above simulation results and Table VI. The comparison of proposed controller performance in

different operating modes is done.

- The fall in voltage below permissible limit happens with exclusion of compensation of reactive power in grid-connected mode as seen in situation 1, Fig. 26 (a). The improvement in voltage profile in middle end of feeders is done by compensation of reactive power depending on confined measurement as shown in situation 2, Fig. 28 But at the far end of the feeders the improvement in the voltage profile is not good. The compensation of suitable reactive power and voltage within permissible limits can be achieved successfully by the proposed controller as described in situation 3, Fig. 31 (a).
- The fall in voltage below permissible limit happens with exclusion of compensation of reactive power in

autonomous mode as described in situation 1, Fig. 27 (a). The improvement in voltage profile is done by compensation of reactive power depending on confined measurement as described in situation 2, Fig. 29(a). The Improvement in voltage profile is further observed by the proposed as described in situation 3, Fig. 32 (a). Compensation of reactive power in situation 3 is achieved better by the proposed controller as described in situation 3, Fig. 33) compared to confined compensation of reactive power as described in situation 2, Fig. 30 (a) in the islanding sequence of operation. The efficient improvement in the voltage profile is observed in operation of grid in autonomous modem by the proposed controller.

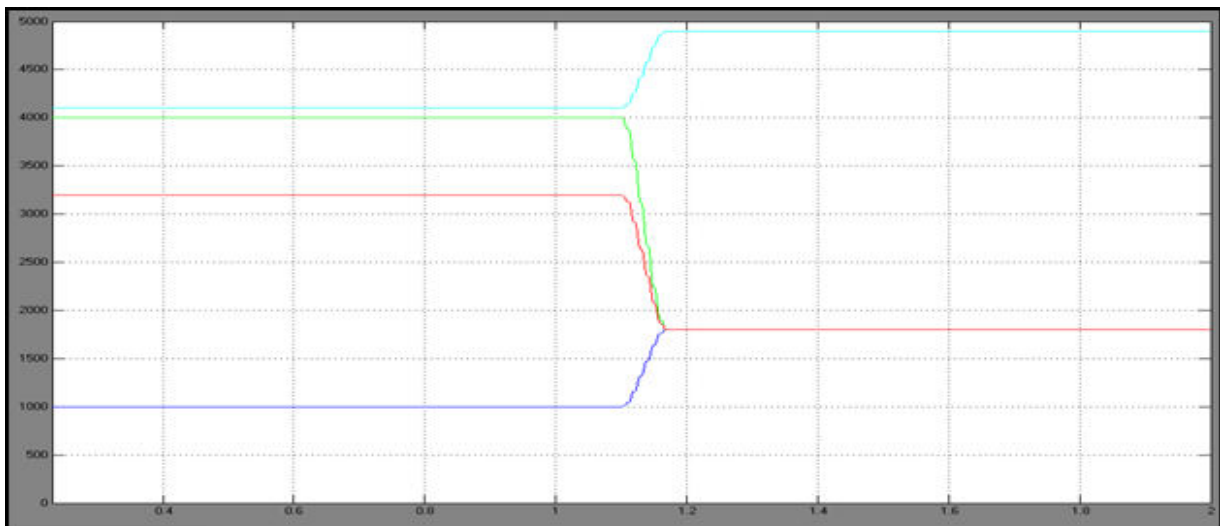


Fig. 25. phase A DGs output power

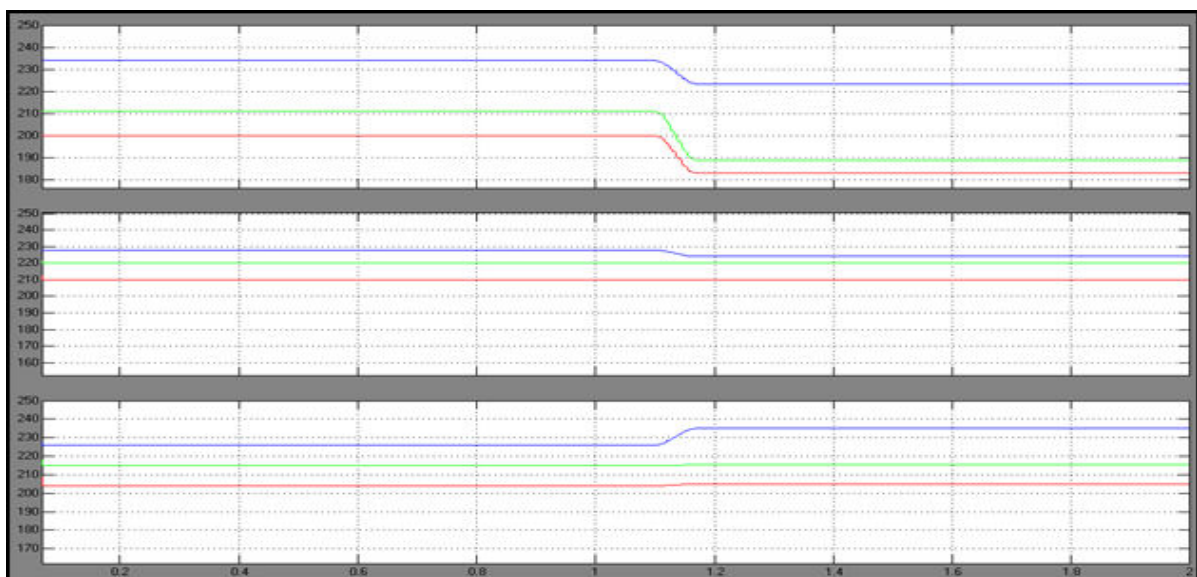
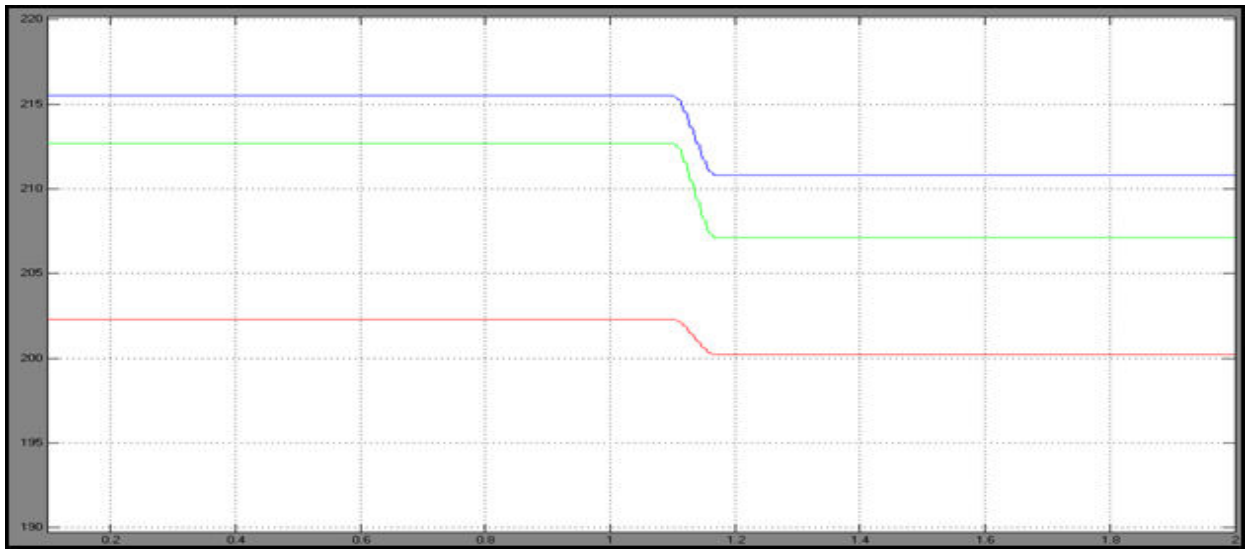
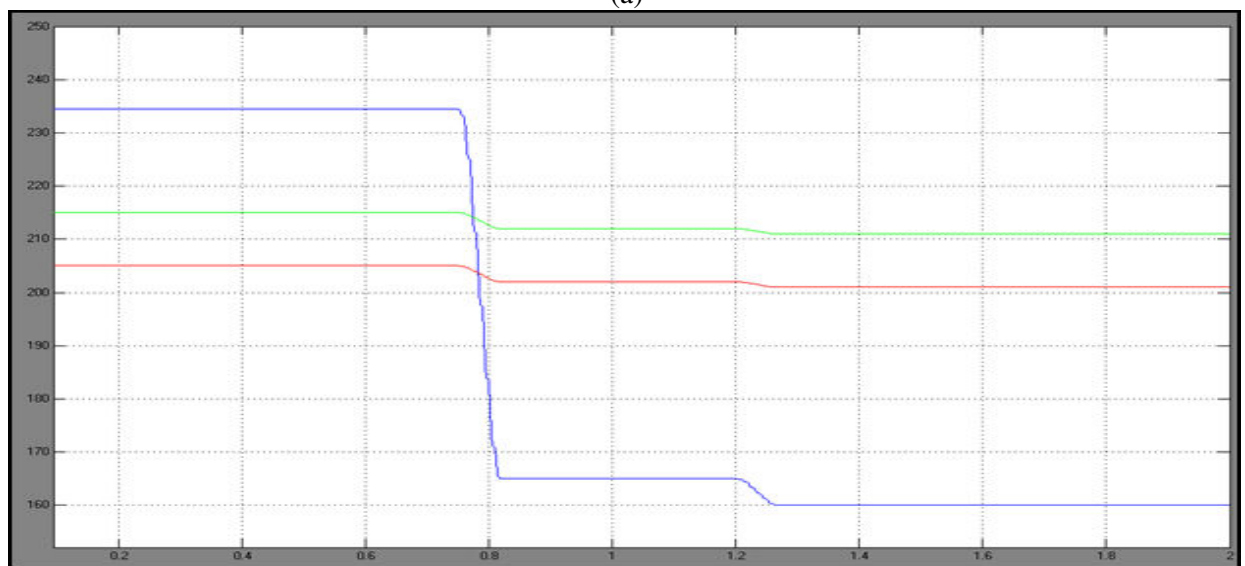


Fig. 26. Different phases RMS voltages. (a) phase A RMS voltages (b) phase B RMS voltages. (c) phase C RMS voltages.





(a)



(b)

Fig. 27. Series-2 and Series-3 describing RMS voltages. (a) Series-2 describing phase A RMS voltages. (b) Series-3 describing phase B RMS voltages.

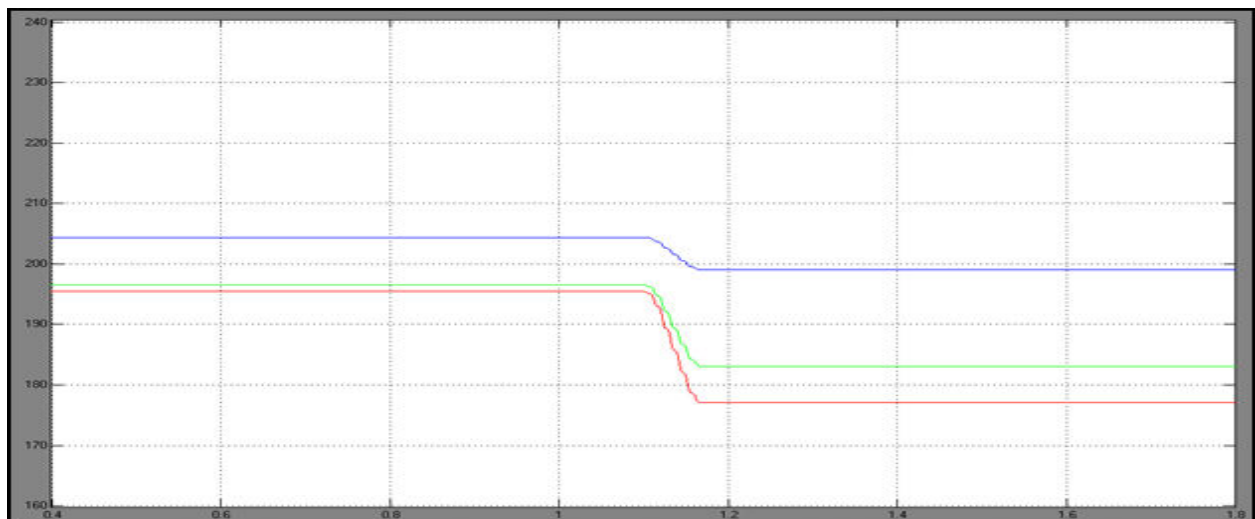
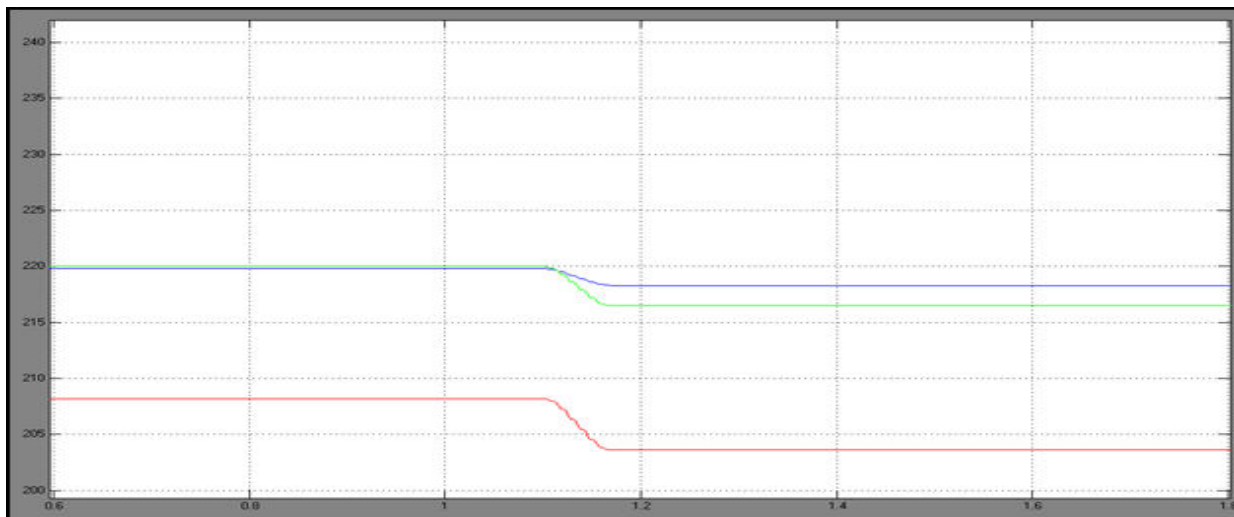
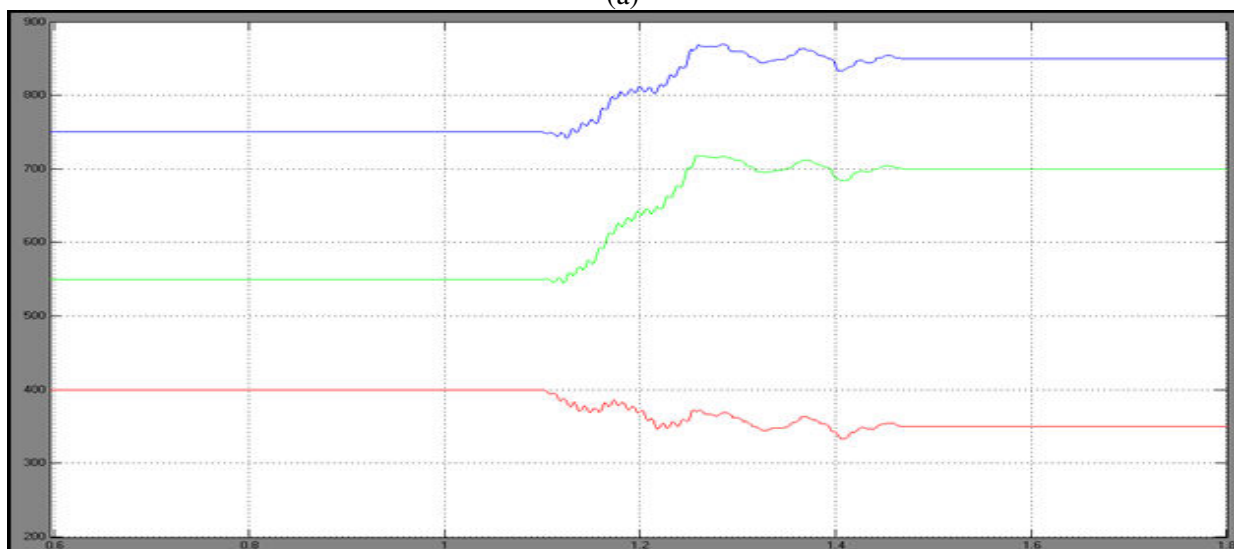


Fig. 28. DSTATCOM describing series-1 phase A RMS voltage

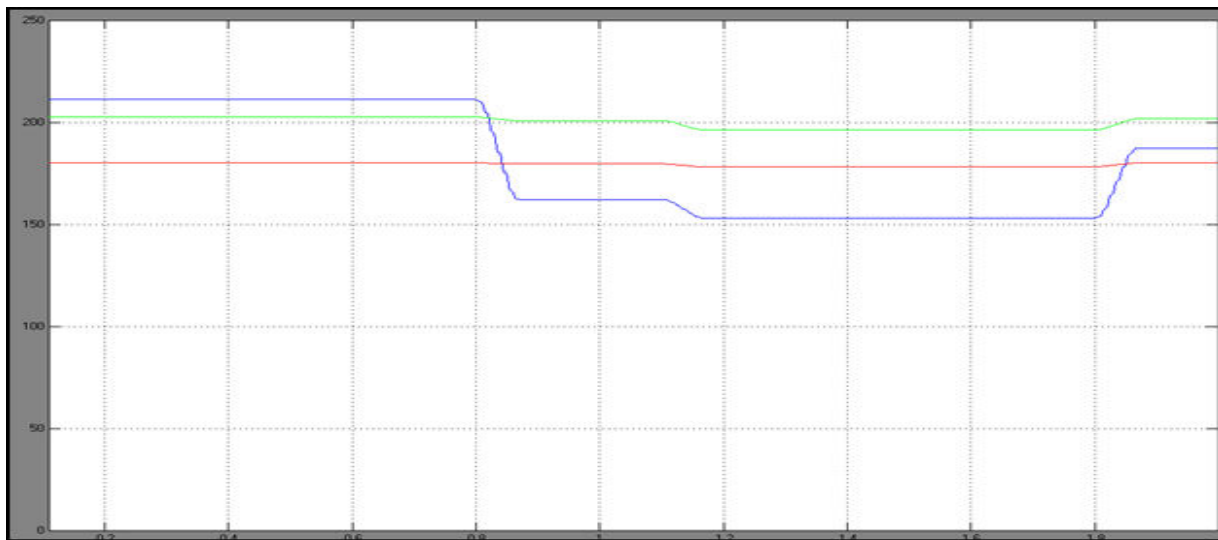


(a)

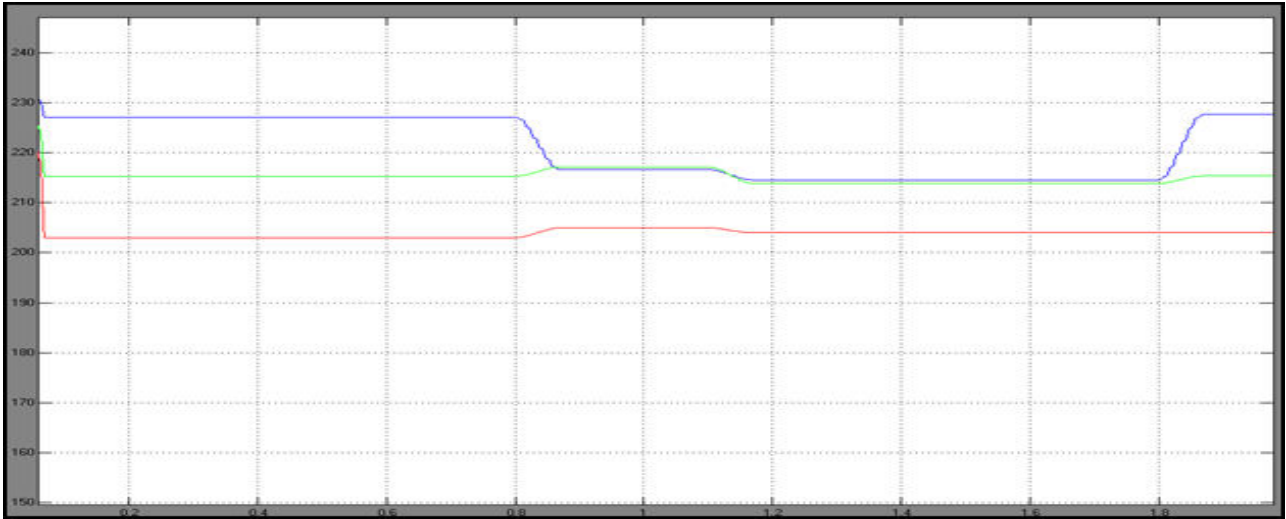


(b)

Fig. 29. Series-2 describing RMS voltages and injection of reactive power. (a) Phase RMS voltages in different location. (b) DSTATCOM describing injection of reactive power three different phases.

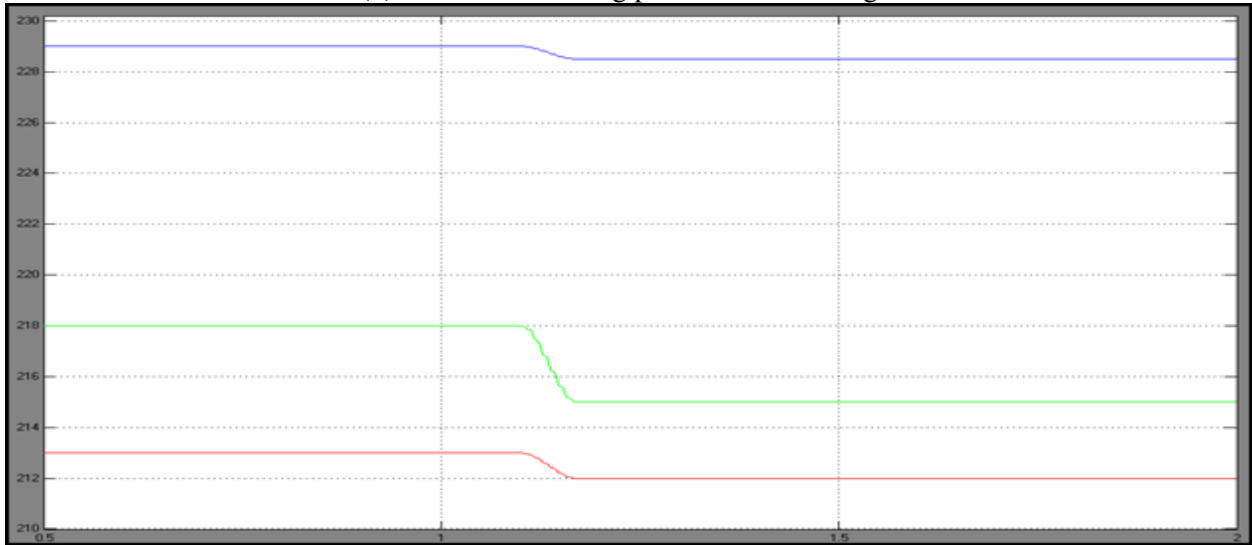


(a)

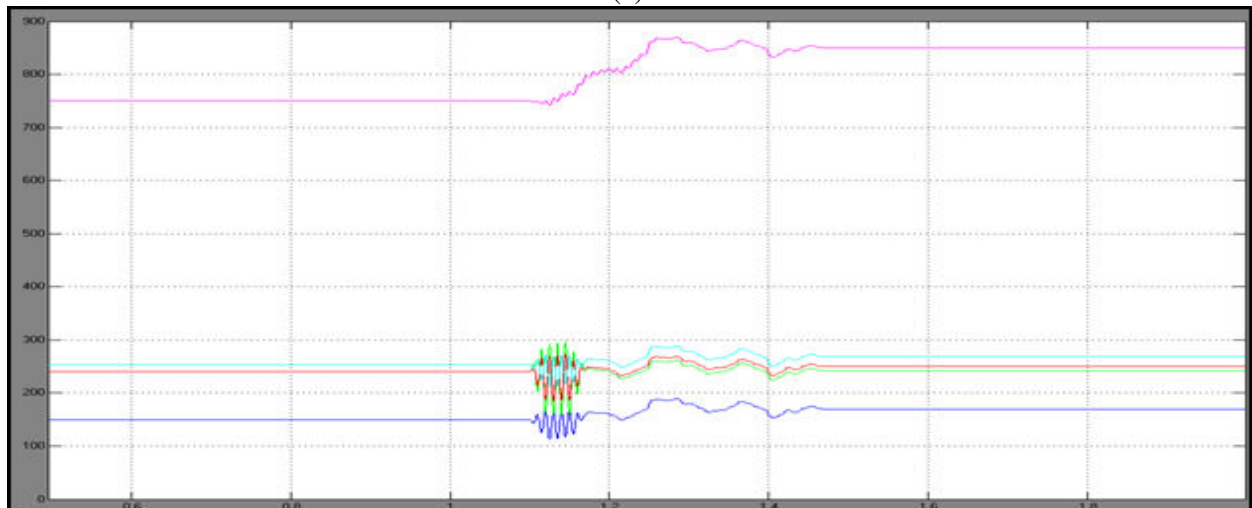


(b)

Fig. 30. Series-3 describing RMS voltages. (a) Series-3 describing phase A RMS voltages.  
(b) Series-3 describing phase B RMS voltages

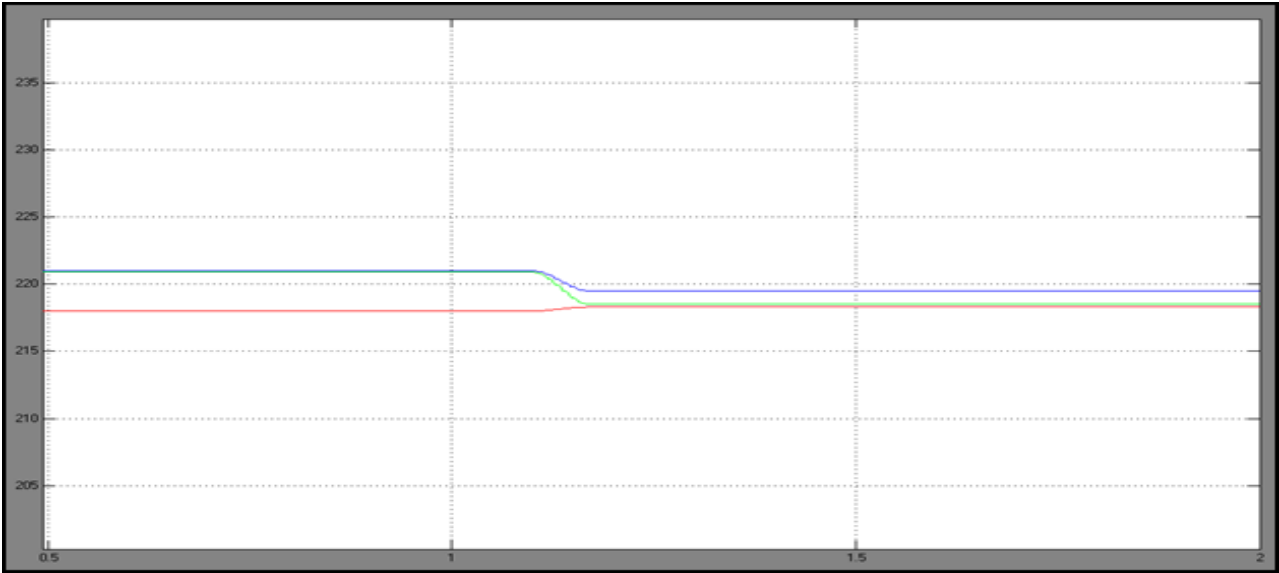


(a)

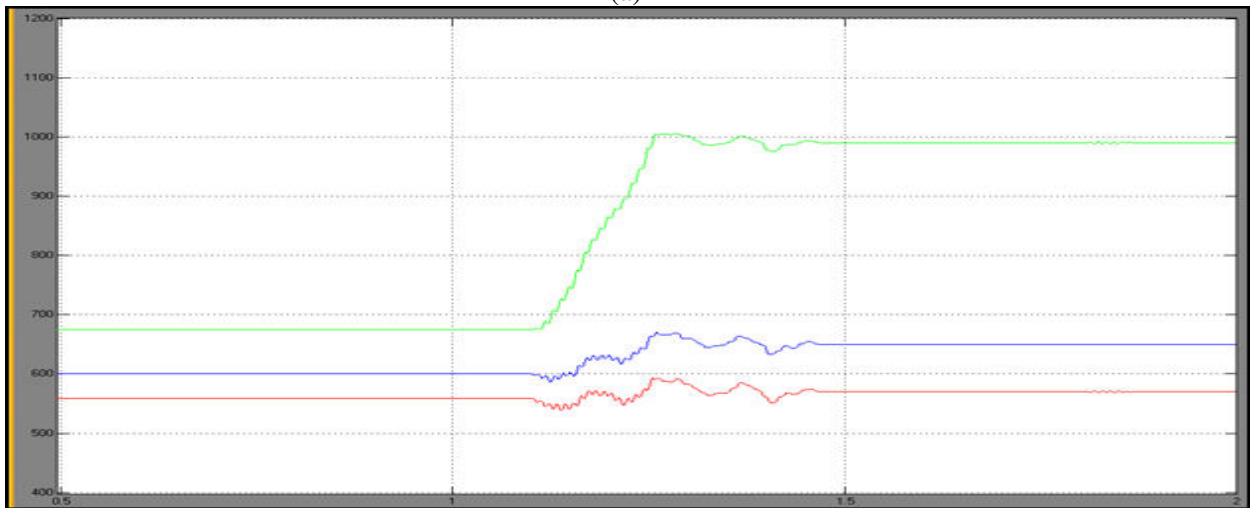


(b)

Fig. 31. Series-1 describing RMS voltages and injection of reactive power. (a) Series-1 describing phase A RMS voltages with the proposed method. (b) DSTATCOM and DG's describing injection of reactive power



(a)



(b)

Fig. 32. Series-2 describing RMS voltages and injection. (a) Series-2 describing phase A RMS voltages. (b) DSTATCOM describing injection of reactive power injection in three phases.

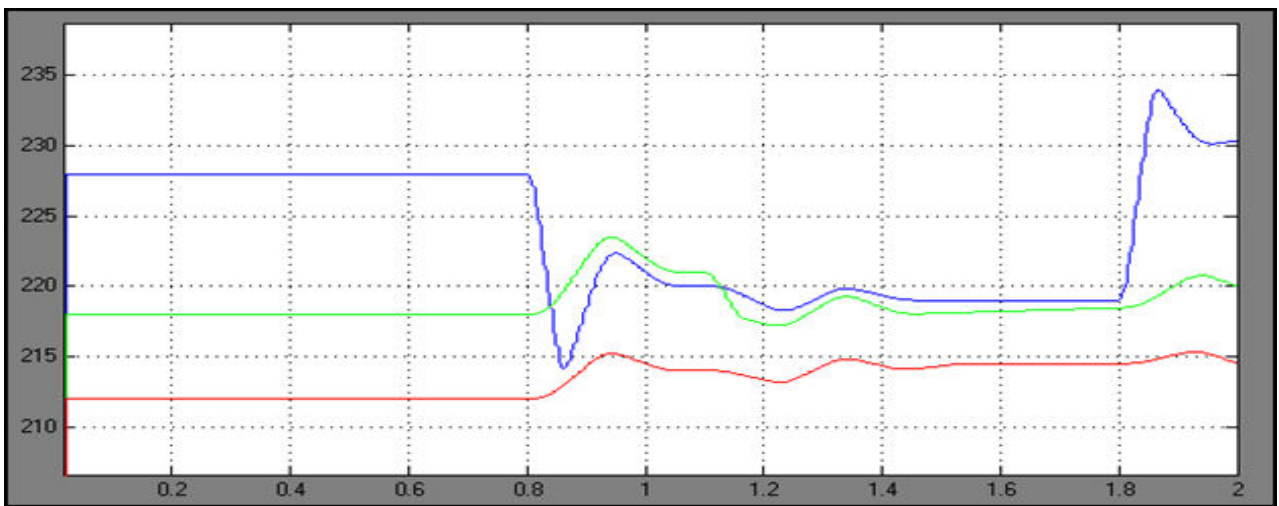


Fig. 33. Series-3 describing phase A RMS voltages

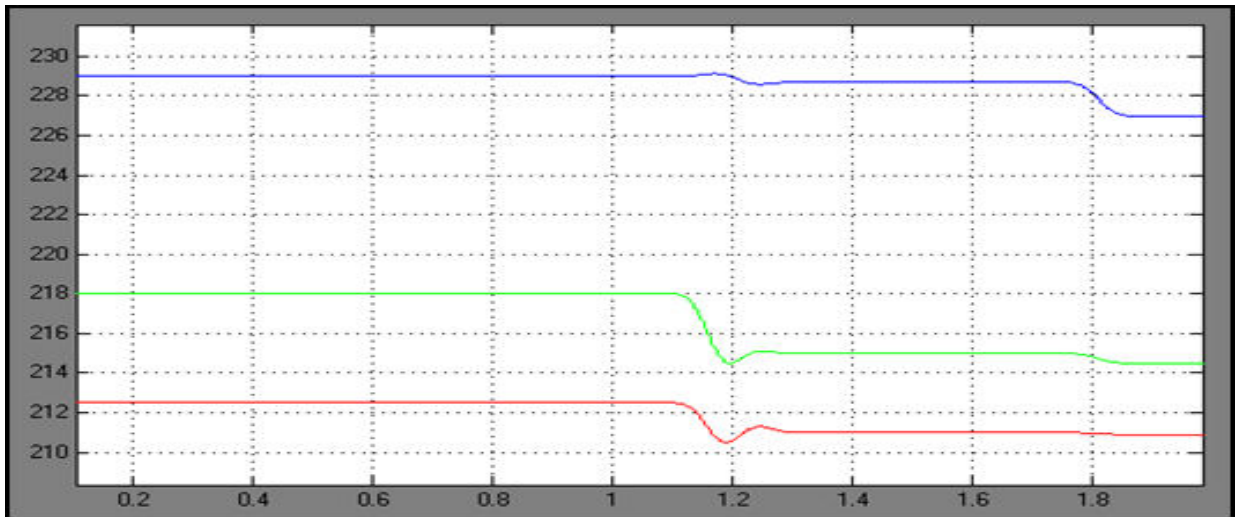


Fig. 34. Series-1 describing phase A RMS voltages at failure of communication node at DG

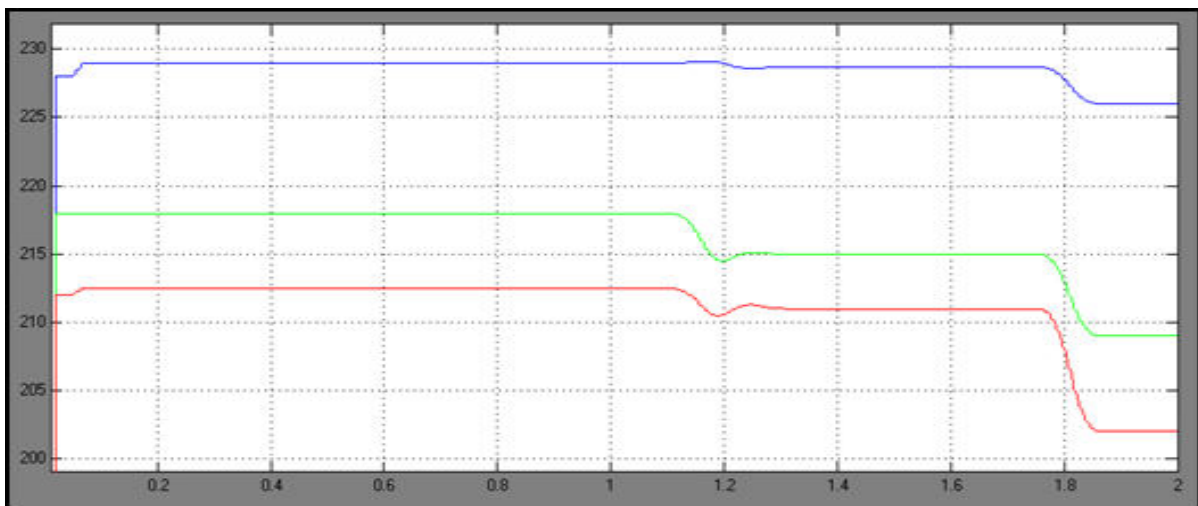


Fig. 35. RMS voltages of phase A in Sq-1 followed by a DSTATCOM node failure

failure of communication node occurred at the utility side of DG as described in situation 4, Fig. 34. Ceasing of communication with all DSTATCOM happened to made very large influence on failure of communication node at DSTATCOM as described in situation 5, Fig. 35.

The absence of DSTATCOM communication has made it just like situation 2 within confined measurements only. The range of reactive limit is achieved and works properly by the adaptation of the DG. Simulation of different situations by proposed method shows the average drop in voltage within permissible limits in all the situations. With absence of compensation the average drop in voltage with modern DSTATCOM, and with the proposed method as described in Fig. 36.

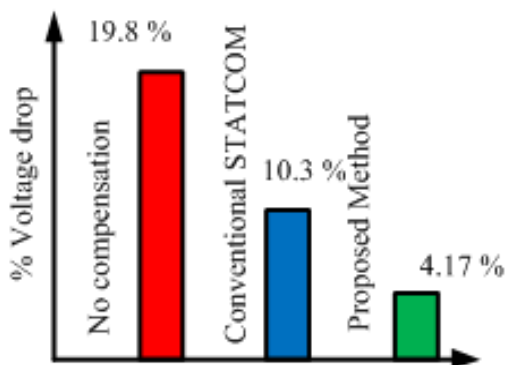


Fig. 36. Drop in average voltage with inclusion and exclusion of reactive compensation

## 7. Conclusion

The operation of DSTATCOM with communication has a new control technique is proposed in this paper. The small communities which are physically far apart are covered by feeders having single phase loads by the application aimed for micro grid. Depending on the line power flow and local measurement, the proposed reactive



compensation is achieved. The voltage regulation is maintained with a large diffusion of DGs by effectively reducing the drop in voltage and is shown by the proposed method. The requirement of transfer of data is verified by the communication set-up for information transfer study. The performance of DSTATCOM is superior under different operating conditions is shown by the simulations of the power network and the communication network in a closed loop.

## REFERENCES

- [1] X. Yoasuo, C. Liuchen, B. K. Soren, B. Josep, and S. Toshihisa, "Topologies of single-phase inverters for small distributed power generators: An overview," *IEEE Trans. Power Electron.*, vol. 19, no. 5, pp. 1305–1314, Sep. 2004.
- [2] T. E. McDermott and R. C. Dugan, "Distributed generation impact on reliability and power quality indices," in *Proc. IEEE Rural Elect. Power Conf.*, 2002, pp. D3\_1–D3\_7.
- [3] National Energy Technology Laboratory, U.S. Department of Energy, *Provides Power Quality for 21st Century Needs*, Jan. 2007.
- [4] 978-1-84800-317-0R. Strezelecki and G. Benysek, "Active power quality controllers," in *Power Electronic in Smart Electrical Energy Network*. New York: Springer-Verlag, 2011.
- [5] R. Majumder, A. Ghosh, G. Ledwich, and F. Zare, "Operation and control of single phase micro-sources in a utility connected grid," in *Proc. IEEE PES*, Jul. 26–30, 2009, pp. 1–7.
- [6] Ch. Rami Reddy, K. Harinadha Reddy "A Passive Islanding Detection method for Neutral point clamped Multilevel Inverter based Distributed Generation using Rate of Change of Frequency Analysis", *International Journal of Electrical and Computer Engineering*, vol. 8, no.4, pp.1967-1976, 2018.
- [7] Z. Tao and B. Francois, "Energy management and power control of a hybrid active wind generator for distributed power generation and grid integration," *IEEE Trans. Ind. Electron.*, vol. 58, no. 1, pp. 95–104, Jan. 2011.
- [8] Z. Qing-Chang and G. Weiss, "Synchronverters: Inverters that mimic synchronous generators," *IEEE Trans. Ind. Electron.*, vol. 58, no. 4, pp. 1259–1267, Apr. 2011.
- [9] Y. Shuitao, L. Qin, F. Z. Peng, and Q. Zhaoming, "A robust control scheme for grid-connected voltage-source inverters," *IEEE Trans. Ind. Electron.*, vol. 58, no. 1, pp. 202–212, Jan. 2011.
- [10] I. J. Balaguer, L. Qin Lei, Y. Shuitao, U. Supatti, and P. Fang Zheng, "Control for grid-connected and intentional islanding operations of distributed power generation," *IEEE Trans. Ind. Electron.*, vol. 58, no. 1, pp. 147–157, Jan. 2011.
- [11] B V Rajanna, Ganta Joga Rao, SK Shrivastava, "Defining Control Strategies for Micro Grids Islanded Operation with Maximum Power Point Tracking using a Fuzzy Logic Control Scheme", *International Journal of Power Electronics and Drive systems*, vol. 7, no. 3, pp: 723-733, Sep. 2016.
- [12] J. M. Guerrero, J. C. Vasquez, J. Matas, M. Castilla, and L. G. de Vicuna, "Control strategy for flexible microgrid based on parallel line-interactive UPS systems," *IEEE Trans. Ind. Electron.*, vol. 56, no. 3, pp. 726–736, Mar. 2009.
- [13] Ch. Rami Reddy, K. Harinadha Reddy "Islanding detection for inverter based distributed generation with Low frequency current harmonic injection through Q controller and ROCOF analysis", *Journal of electrical systems*, volume: 14, issue: 02, pp: 179-191, 2018.
- [14] T.Sauter and M. Lobashov, "End-to-end communication architecture for smart grids," *IEEE Trans. Ind. Electron.*, vol. 58, no. 4, pp. 1218–1228, Apr. 2011.
- [15] P. Rodríguez, A. Luna, I. Candela, R. Mujal, R. Teodorescu, and F. Blaabjerg, "Multiresonant frequency-locked loop for grid synchronization of power converters under distorted grid conditions," *IEEE Trans. Ind. Electron.*, vol. 58, no. 1, pp. 127–138, Jan. 2011.
- [16] B V Rajanna, K S srikanth "Grid Connected Inverter for Current Control Using Anti Islanding Technique", *International journal of power electronics and drive systems*, vol. 9, no. 2, pp: 926-932, Jun. 2018.
- [17] *IEEE Application Guide for IEEE Std 1547, IEEE Standard for Interconnecting Distributed Resources With Electric Power Systems*, IEEE Std. 1547.2-2008, Apr. 15, 2009. doi: 10.1109/IEEESTD.2008.4816078, pp. 1–207.
- [18] L. Tzung-Lin, H. Shang-Hung, and C. Yu-Hung, "Design of D-STATCOM for voltage regulation in micro grids," in *Proc. IEEE ECCE*, Sep. 12–16, 2010, pp. 3456–3463.
- [19] R. Majumder, A. Ghosh, G. Ledwich, and F. Zare, "Enhancing the stability of an autonomous microgrid using DSTATCOM," *Int. J. Emerg. Elect. Power Syst.*, vol. 10, no. 5, pp. 1–23, Dec. 2009.
- [20] R. Majumder, G. Ledwich, A. Ghosh, S. Chakrabarti, and F. Zare, "Droop control of converter-interfaced microsources in rural distributed generation," *IEEE Trans. Power Del.*, vol. 25, no. 4, pp. 2768–2778, Oct. 2010.
- [21] Ch. Rami Reddy, K. Harinadha Reddy "Islanding detection method for inverter based distributed generation based on combined changes of ROCOAP and ROCORP", *International journal of pure and applied mathematics*, vol: 117(19), pp: 433-440, 2017.
- [22] B. Singh, A. Adya, A. P. Mittal, and J. R. P. Gupta, "DSTATCOM for power quality improvement in a four-wire electric distribution system," *Int. J. Global Energy Issues*, vol. 26, no. 3/4, pp. 401–416, 2006.
- [23] G. Ledwich and A. Ghosh, "A flexible DSTATCOM

- operating in voltage or current control mode,” *Proc. Inst. Elect. Eng.—Gen., Transm. Distrib.*, vol. 149, no. 2, pp. 215–224, Mar. 2002
- [24] National Energy Technology Laboratory, US Department of Energy, Office of Energy Delivery and Energy Reliability, *Integrated Communications-A System View of Modern Grid*, Feb. 2007.
- [25] R. Majumder, “Modeling, Stability Analysis and Control of Microgrid,” Ph.D. dissertation, Queensland Univ. Technol., Brisbane, Australia, 2010.
- [26] S G Prasad, K S Srikanth, B V Rajanna, “Advanced Active Power Filter Performance for Grid Integrated Hybrid Renewable Power Generation Systems”, *Indonesian Journal of Electrical Engineering and Computer Science*, vol. 11, no. 1, pp. 60-73, Jul. 2018.
- [27] Rami reddy, K. Harinadha reddy “Islanding detection with DQ transformation based PI approach in distributed generation” *International journal of control theory and applications*, volume 5(10)-2017.
- [28] Sung Min Park; Sung-Yeul Park “Versatile unidirectional AC-DC converter with harmonic current and reactive power compensation for smart grid applications” *IEEE Applied Power Electronics Conference Exposition 2014*, Pp: 2163 - 2170, 2014.
- [29] Xiao Luo; Chi Kwan Lee; Wai Man Ng; Shuo Yan; Balarko Chaudhuri; Shu Yuen Ron Hui “Use of Adaptive Thermal Storage System as Smart Load for Voltage Control and Demand Response” *IEEE Transactions on Smart Grid*, Volume: 8, Issue: 3 Pages: 1231 - 1241, Year: 2017.
- [30] Ahsan Shahid “Power quality control in grid-interactive micro-power systems” *2016 IEEE International Conference on Renewable Energy Research and Applications*, Pages: 966 - 970, 2016.
- [31] Yan Li; Jinli Zhao; Zhelin Liu; Peng Li; Xin Zhang; Xiaojun Tang “Assessment method of dynamic reactive power valuation for transient voltage stability” *2013 IEEE International Conference of IEEE Region 10*, Pages: 1 - 4, Year: 2013.
- [32] Yong-Jun Zhang; Shu-Yi Sun; Xiang-Min Huang “The decoupled control of reactive power in medium/low voltage distribution networks including distributed generation” *2015 International Conference on Smart Grid and Clean Energy Technologies (ICSGCE)*, Pages: 129.133, Year: 2015.
- [33] Mareio M. de Oliveira; Mikael Halonen “Dynamic reactive power compensation: Opportunities and challenges in the mexican grid” *2016 IEEE PES Transmission & Distribution Conference and Exposition-Latin America* pp: 1 - 6, Year: 2016.
- [34] Naga Brahmendra Yadav Gorla; Kawsar Ali; Chia Chew Lin; Sanjib Kumar Panda “Improved utilization of grid connected voltage source converters in smart grid through local VAR compensation” *IECON 2015 - 41<sup>st</sup> Annual Conference of the IEEE Industrial Electronics Society*, Pages: 002532002537, Year: 2015.
- [35] Pinkymol Harikrishna Raj; Ali I. Maswood; Gabriel H. P. Ooi; Hossein Dehghani Tafti “Five-level multiple-pole mutli level diode-clamped inverter scheme for reactive power compensation” *2015 IEEE Innovative Smart Grid Technologies*, PP: 5, 2015.
- [36] K. V. Siva Reddy, SK. Moulali, K. Harinadha Reddy, Ch. Rami Reddy, B. V. Rajanna, G. Venkateswarlu, Ch. Amarendra “Resonance Propagation and Elimination in Integrated and Islanded Micro grids”, *International journal of power electronics and drive systems*, vol. 9, no. 3, pp. 1445-1456, Sep. 2018.
- [37] Nabil Akel; Tom Bowker; Victor Goncalves “Dual-purposing telecom backup systems for cloud energy storage and grid ancillary services” *2014 IEEE 36th International Telecommunications Energy Conference (INTELEC)*, Pages: 1.4, Year: 2014
- [38] Saverio Bolognani; Ruggero Carli; Guido Cavraro; Sandro Zampieri “A distributed control strategy for optimal reactive power flow with power and voltage constraints” *2013 IEEE International Conference on smart grid communications*, Pages: 115-120, Year: 2013.
- [39] Chenye Wu; Hamed Mohsenian-Rad; Jianwei Huang “PEV based reactive power compensation for wind DG units A stackelberg game approach” *2012 IEEE Third International Conference on Smart Grid Communications*, Pp: 504-509, 2012.
- [40] Fuka Ikeda; Kei Nishikawa; Hiroaki Yamada; Toshihiko Tanaka; Masayuki Okamoto “Constant DC-capacitor voltage control based strategy for harmonics compensation of smart charger for electric vehicles in single-phase three-wire distribution feeders with reactive power control” *IEEE Energy Conversion Congress and Exposition*, Pp: 1-7, Year: 2016.
- [41] Saverio Bolognani; Ruggero Carli; Guido Cavraro; Sandro Zampieri “Distributed Reactive Power Feedback Control for Voltage Regulation and Loss Minimization”, *IEEE Transactions on Automatic Control*, Volume: 60, Issue: 4, Pages: 966-98, 2015.
- [42] A. S. Maklakov; A. A. Radionov “Integration prospects of electric drives based on back to back converters in industrial smart grid” *2014 12th International Conference on Actual Problems of Electronics Instrument Engineering* Pages: 770.774, Year: 2014.
- [43] T. Bharath Kumar; M. Venu Gopala Rao “Mitigation of Harmonics and power quality enhancement for SEIG based wind farm using ANFIS based STATCOM” *2014 International Conference on Smart Electric Grid*, Pages: 1-7, Year: 2014.
- [44] Ch Rami Reddy, K Harinadha Reddy, K Venkata Siva Reddy “Recognition of Islanding Data for Multiple Distributed Generation Systems with ROCOF Shore Up Analysis”, *Smart Intelligent Computing and Applications*, pp: 547-558, 2019.
- [45] B. V. Rajanna, Ch. Rami Reddy, K. Harinadha Reddy “Design, Modeling & Simulation of DSTATCOM for Distribution Lines for Power Quality Improvement”, *Journal of Electrical Engineering*, vol. 17, no.2, pp. 1-10, 2017.